Check for updates

JGR Oceans

RESEARCH ARTICLE
10.1029/2025JC023603

Oceanographic Drivers of Larval Transport Variability in South Atlantic *Jasus paulensis* Populations

E. F. Young[1], S. A. Morley[1], J. B. Bell[2], V. Laptikhovsky[2], J. Glass[3], and M. A. Collins[1]

[1]British Antarctic Survey, Cambridge, UK, [2]Centre for Environment, Fisheries and Aquaculture Science, Suffolk, UK, [3]Fisheries Department, Tristan da Cunha Government, Edinburgh of the Seven Seas, UK

Key Points:

- Lobster population at Gough Island (GI) is dependent on retention of locally produced larvae
- Variability in the retention of locally produced larvae at the northern islands is moderated by inputs of larvae from GI
- Stronger and more frequent El Niño events are likely to negatively impact lobster populations

Supporting Information:

Supporting Information may be found in the online version of this article.

Correspondence to:

E. F. Young,
eyoung@bas.ac.uk

Citation:

Young, E. F., Morley, S. A., Bell, J. B., Laptikhovsky, V., Glass, J., & Collins, M. A. (2026). Oceanographic drivers of larval transport variability in South Atlantic *Jasus paulensis* populations. *Journal of Geophysical Research: Oceans*, *131*, e2025JC023603. https://doi.org/10.1029/2025JC023603

Received 15 OCT 2025
Accepted 25 JUN 2026

Author Contributions:

Conceptualization: E. F. Young, S. A. Morley
Formal analysis: E. F. Young
Funding acquisition: S. A. Morley
Investigation: E. F. Young
Methodology: E. F. Young
Resources: S. A. Morley
Software: E. F. Young
Writing – original draft: E. F. Young
Writing – review & editing: S. A. Morley, J. B. Bell, V. Laptikhovsky, J. Glass, M. A. Collins

© 2026. The Author(s).
This is an open access article under the terms of the Creative Commons Attribution License, which permits use, distribution and reproduction in any medium, provided the original work is properly cited.

Abstract Effective fisheries management requires an understanding of the key influences on population variability. A fundamental driver of variability, particularly for isolated island populations, is the transport of planktonic early-life stages. Here, we use numerical modeling tools to investigate the role of oceanographic variability in the transport of *Jasus paulensis* (Tristan rock lobster) larvae in the southeast Atlantic. Model simulations highlight a lack of upstream sources for populations at the Tristan da Cunha (TdC) archipelago, suggesting a dependence on local retention and regional-scale transport between the islands. Model results indicate that years with poor retention in the northern island group are moderated by regular imports of larvae from Gough Island (GI), which suggests greater reliability in larval supply to the northern island group. However, GI rarely receives imports of larvae from elsewhere and the population is therefore dependent on retention of locally produced larvae. Periods of stronger eastward flows through the region, driven by stronger northerly and westerly winds, are associated with broadly reduced larval retention throughout the archipelago, and reduced northward export of larvae from GI, although the response at the northern island group is mixed and dependent on the timing of the strengthened flows. These results suggest that periods of stronger westerly winds through more frequent and intense El Niño events may have a negative impact on *J. paulensis* populations in the Tristan archipelago. Our findings provide insight into regional population connectivity dynamics and responses to environmental variability and change, to support management of the *J. paulensis* fishery.

Plain Language Summary The economy of the remote archipelago of Tristan da Cunha in the South Atlantic is largely reliant on fishing, in particular the Tristan rock lobster. Therefore, it is important to ensure long-term sustainability of the fishery through effective management practices. This requires an understanding of factors that influence the size of the fishable stock, including the transport and retention of the long-lived pelagic larvae. In this study, we used a numerical modeling approach to investigate how variability in ocean currents in the South Atlantic impacts larval transport. We found that larvae transported to Gough Island (GI) in the south of the archipelago are mostly spawned locally, whereas those arriving at the northern islands are spawned both locally and at GI. However, there was large variability in successful transport and retention between years partly driven by variability in regional winds. Periods with stronger northerly and westerly winds tend to result in reduced larval supply to islands throughout the archipelago. In the future, periods of stronger westerly winds may increase due to more frequent and intense El Niño events, which could have a negative impact on Tristan rock lobster populations in the Tristan da Cunha archipelago.

1. Introduction

Effective management of marine ecosystems is critical for maintaining the health and sustainability of oceanic biodiversity and the services these ecosystems provide. Over the past few decades, human activities such as overfishing, pollution, and habitat destruction have significantly impacted marine environments, leading to the degradation of key ecosystems and the loss of biodiversity (Halpern et al., 2008). Sustainable management practices, including the establishment of Marine Protected Areas or Zones (MPAs or MPZs) and the setting of catch limits based upon abundance indices and reference points derived from life history information, are essential for reversing these trends and promoting resilience (Lubchenco et al., 2003; Micheli et al., 2012; Sala & Giakoumi, 2018). Such management activities are increasingly used as tools to protect marine environments and range from fully protected no-take zones to multiple-use areas that permit sustainable fishing and other activities (Agardy, 1997; Oregon State University, IUCN World Commission on Protected Areas—Marine, Marine Conservation Institute, National Geographic Pristine Seas, and UN Environment Programme World Conservation Centre, 2023). Sustainable management of marine resources is particularly important for small island states

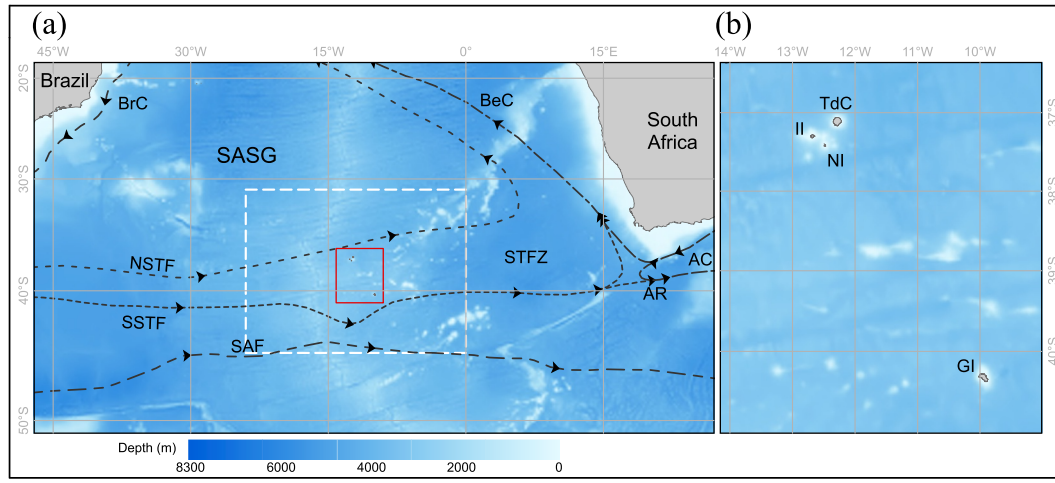

Figure 1. (a) Location of the Tristan da Cunha (TdC) archipelago in the South Atlantic (red box) with a schematic illustration of major oceanographic features and associated direction of flows: South Atlantic Subtropical Gyre (SASG), Subantarctic Front (SAF), Southern Subtropical Front (SSTF), Northern Subtropical Front (NSTF), Subtropical Frontal Zone (STFZ), Brazil Current (BrC), Benguela Current (BeC), Agulhas Current (AC), Agulhas Retroflection (AR). The regional model domain is shown by the white dashed box. The extracted region in (b) is shown by the red box. (b) Islands of the TdC archipelago: Gough Island (GI) and the northern island group, TdC, Inaccessible Island (II) and Nightingale Island (NI). Bathymetry (blue shading) is extracted from the General Bathymetric Chart of the Oceans 2025 grid (GEBCO Compilation Group, 2025).

whose food security, economy, and cultural identity often rely on the health of their marine environment (Hay, 2013; Vye et al., 2024).

Tristan da Cunha (TdC), part of the UK Overseas Territory of St Helena, Ascension and TdC, is one such remote archipelago located in the South Atlantic. The TdC island group consists of two archipelagos of volcanic islands; the largest (the northern group) encompasses Tristan, Nightingale and Inaccessible Islands, and Gough Island (GI) lies approximately 400 km southeast of the northern group (Figure 1). The economy of TdC is largely dependent on fishing, in particular exports of Tristan rock lobster (*J. paulensis*; marketed as *J. tristani*). The fishery is a combination of local vessels around the northern islands and larger vessels that fish at both the northern island group and at GI. The fishery typically produces around 400–450 metric tonnes of lobster (whole and tails) per year, and has had Marine Stewardship Council sustainability certification continuously since 2011 (Blamey et al., 2019; Sánchez-Llamas & Groeneveld, 2025).

Recruitment, which, in the parlance of fisheries science, means the number of new individuals that become accessible to a fishery each year, is often highly stochastic. This variability is a combination of larval transport to a given stock area, and survival to a certain age or size. It is most pronounced when there is an extended pelagic larval phase and has a major influence on the long-term productivity of a given stock (Fogarty et al., 1991; Myers & Pepin, 1994). Recruitment, in this sense, is generally difficult or even impossible to predict accurately, and factors such as ocean currents, water temperature (particularly including the timing and severity of marine heatwaves; e.g. Marochi et al., 2022), and habitat availability and condition all influence recruitment success (Caputi et al., 1996). Understanding such processes is essential to support more accurate stock assessments, set sustainable catch limits, and thus enhance the resilience of marine populations and promote long-term sustainability. This is particularly important for remote oceanic island groups such as TdC where larvae have the potential to drift significant distances away from the islands on which they are spawned. Understanding the processes that lead to larvae being retained or, if very few are retained, where successful recruits may come from, is key to long-term sustainable management of marine resources, especially in areas that are remote from suitable habitats elsewhere.

Tristan lobster (previously *J. tristani*) was considered endemic to the South Atlantic, with populations limited to the TdC archipelago and Vema Seamount (~2,000 km to the northeast); however, analyses of mitochondrial DNA showed little to no genetic differentiation between *J. tristani* and the St Paul rock lobster, *J. paulensis*, found in the southern Indian Ocean and suggested that *J. paulensis* and *J. tristani* should be synonymized as *J. paulensis* (Groeneveld et al., 2012). However, the existence of morphological differences (George & Kensler, 1970) and the

21699291, 2026, 7, Downloaded from https://agupubs.onlinelibrary.wiley.com/doi/10.1029/2025JC023603 by British Antarctic Survey, Wiley Online Library on [23/07/2026]. See the Terms and Conditions (https://onlinelibrary.wiley.com/terms-and-conditions) on Wiley Online Library for rules of use; OA articles are governed by the applicable Creative Commons License

identification of a low but significant genetic differentiation using neutral single-nucleotide polymorphisms (Silva et al., 2021) support a degree of isolation between the two stocks or putative sub-species. Further, while large-scale numerical modeling confirmed a weak and inconsistent eastward connectivity from the TdC archipelago to St Paul Island, model simulations predicted no direct westward transport. Together, these studies suggest that *J. paulensis* populations in the South Atlantic are dependent on the regional retention or return of locally produced larvae (Silva et al., 2021).

Adult *J. paulensis* mainly inhabit shallow rocky reefs at depths from the intertidal zone to ~200 m (Glass, 2014). Spawning starts in the austral autumn (May) and females carry externally fertilized eggs during winter (Roscoe, 1979), with hatching into planktonic phyllosoma larvae peaking in early spring. The pelagic larval duration of *J. paulensis* phyllosoma is not known but likely to be long; the observed duration for other *Jasus* species is 7–22 months (George, 2005). At the end of the phyllosoma stage, the larvae molt into a short-lived puerulus stage that settles inshore and, after a few days, molts into the first juvenile phase (Glass, 2014). The puerulus of *Jasus* species is a non-feeding stage; therefore, for successful settlement, metamorphosis to the inshore habitat must occur within the swimming range of the puerulus (Chiswell & Booth, 2017).

During the long planktonic phyllosoma stage, larvae may be dispersed considerable distances by ocean currents. For example, the long larval duration of *Jasus edwardsii* combined with large-scale prevailing currents has been postulated to drive connectivity between adult populations thousands of kilometres apart (Chiswell et al., 2003). However, oceanographic features such as fronts and eddies can also restrict larval transport between proximate locations (Young et al., 2015). Alternatively, such features may act to retain larvae close to their point of origin or return them to coastal habitats after being dispersed far offshore (Chiswell & Booth, 1999). The TdC archipelago lies within the Subtropical Frontal Zone (STFZ) in the southern limb of the South Atlantic subtropical gyre (SASG; Figure 1). The STFZ is bounded to the north and south by the Northern and Southern Subtropical Fronts (NSTF and SSTF; Belkin & Gordon, 1996) and is characterized by enhanced sea surface temperature (SST) gradients but weak gradients in sea surface height due to density-compensating salinity gradients (Graham & De Boer, 2013). The broadly east to north-eastward flows within the STFZ have been termed the South Atlantic Current; however, observations suggest that flows are concentrated in jets associated with the NSTF and SSTF, and currents between the fronts are not consistently eastward (Smythe-Wright et al., 1998). The regional oceanography is characterized by a high degree of spatial and temporal variability with seasonal and interannual variability in the latitudinal positions of the NSTF and SSTF, and in the strength of the associated flows (Burls & Reason, 2006; Drouin et al., 2021; Smythe-Wright et al., 1998). Over longer timescales, there has been a southward displacement of the SASG, estimated at 0.11° per decade, coupled with a poleward shift of extra-tropical atmospheric circulation due to anthropogenically driven climate change (Yang et al., 2020). Model predictions suggest that future climate change will drive an increase in the strength of the SASG (Marcello et al., 2023), although analyses of satellite data have found no evidence of an increasing trend over recent decades (Drouin et al., 2021).

Temporal and spatial changes in currents in the southeast Atlantic have the potential to significantly impact the transport of planktonic *J. paulensis* larvae. For example, genetic analyses have suggested that the weak present-day eastward connectivity between populations of *J. paulensis* in the Atlantic and Indian Oceans was reversed in the past, with shifts in basin-scale currents likely playing a role (Silva et al., 2021). Sampling programmes found a wide distribution of *J. paulensis* larvae to the east and northeast of the TdC archipelago, in accordance with the broad east to north-eastward currents in the region (Pollock, 1991), but the mechanism for such larvae to return to the Tristan archipelago is unclear. The presence of low densities of larvae at sampling stations to the west of the islands led Pollock (1991) to infer that the Tristan archipelago may be receiving its supply of puerulus (late stage) larvae via the large-scale currents of the SASG. However, this would require an improbably long larval period of at least 3 years (Glass, 2014); thus, it is more likely that the local population is dependent on transport and retention of larvae within a regional current system. There is a small amount of regular ship transport between the northern island group and GI, and although some degree of larval transport via ballast water exchange is possible, this is not considered a significant mediator of larval connectivity between the islands.

Effective management of the *J. paulensis* fishery requires a comprehensive understanding of the drivers of recruitment variability, including the impact of dispersal and retention of the planktonic larvae. Here, we describe a numerical modeling study of *J. paulensis* larval transport for the TdC archipelago, where successful transport is defined as the transport of larvae to locations of known populations within an appropriate time frame. Using a

21699291, 2026, 7, Downloaded from https://agupubs.onlinelibrary.wiley.com/doi/10.1029/2025JC023603 by British Antarctic Survey, Wiley Online Library on [23/07/2026]. See the Terms and Conditions (https://onlinelibrary.wiley.com/terms-and-conditions) on Wiley Online Library for rules of use; OA articles are governed by the applicable Creative Commons License

21699291, 2026, 7, Downloaded from https://agupubs.onlinelibrary.wiley.com/doi/10.1029/2025JC023603 by British Antarctic Survey, Wiley Online Library on [23/07/2026]. See the Terms and Conditions (https://onlinelibrary.wiley.com/terms-and-conditions) on Wiley Online Library for rules of use; OA articles are governed by the applicable Creative Commons License

combination of basin-scale and high-resolution regional modeling, we ascertain the dominant transport patterns for larvae released at the islands, and the likely pathways for successful transport. Variability in return transport to the natal site (hereafter, retention) and inter-island exchange of larvae is considered, and the results are considered in the context of management of the *J. paulensis* fishery.

2. Methods

An individual-based modeling (IBM) approach was used to investigate the main dispersal pathways for *J. paulensis* larvae spawned at the TdC archipelago, and levels of connectivity between GI, the northern island group, and Vema Seamount. Model simulations were conducted over two geographical scales using flow fields extracted from a global model and a high-resolution nested regional oceanographic model. Large-scale modeling aimed to investigate broad patterns of larval transport and connectivity at the basin scale, including the possibility of large-scale anticyclonic transport in the SASG, which has been suggested previously as a large-scale larval transport mechanism (Pollock, 1991). High-resolution regional modeling aimed to investigate in more detail the influence of smaller-scale mesoscale circulation features on larval transport in the TdC archipelago region; such features are not sufficiently resolved in the larger-scale model.

2.1. Large-Scale Oceanographic Model

Large-scale IBM simulations used velocity fields from a 1/12° global application of the NEMO framework (Nucleus for European Modelling of the Ocean; http://www.nemo-ocean.eu) provided by the National Oceanography Centre, Southampton. The ability of the 1/12° configuration to represent key oceanographic features has been demonstrated (e.g., Deshayes et al., 2013; Marzocchi et al., 2015; Sérazin et al., 2015); full details of the model may be found in Marzocchi et al. (2015). In summary, the model run was started from rest in 1978 and initialized from the World Ocean Atlas 2005 climatological fields. The simulation was forced by 6-hourly winds, daily heat fluxes, and monthly precipitation fields derived from the DFS5.2 reanalysis (Dussin et al., 2016). The model configuration comprised 75 vertical partial z-step levels with variable cell depth such that vertical resolution was higher in the upper water column. The three-dimensional flow fields used in this study comprised 5-day mean velocities for the period 2000 to 2011 for a region encompassing the South Atlantic and southwest Indian Oceans.

2.2. Regional-Scale Oceanographic Model

To investigate fine-scale transport processes in the TdC region, a regional application of NEMO was developed, one-way nested within the 1/12° global model described previously. This includes a realistic representation of the complex local bathymetry derived from the GMRTv3.5 gridded bathymetry (Ryan et al., 2009) with additional high-resolution data incorporated around TdC that was collected in 2018 during cruise JR17-004 on the RRS *James Clark Ross* (Morley et al., 2018). The model domain extends from 45°S to 31°S, and from 24°W to 0°W (Figure 1a), with a horizontal resolution of 1/30° longitude by 1/40° latitude (~3 km), and with 75 vertical levels arranged on a partial z-step coordinate, matching the vertical coordinates of the 1/12° model. For consistency with the 1/12° global model, atmospheric forcing is derived from the DFS5.2 reanalysis (Dussin et al., 2016). At the open boundaries, tides are imposed using the Oregon State University global ocean tide model, TPXO7.2 (Egbert & Erofeeva, 2002). Three-dimensional temperature and salinity, barotropic flux, and sea surface height at the open boundaries are derived from the 1/12° global model. Comparisons with in situ and satellite-derived data (Text S1 in Supporting Information S1) demonstrate that the regional model captures the key features of the observed oceanography in the TdC region. Model fields were stored as 5-day means, including three-dimensional ocean velocities, for 1992–2012; velocities for the period 2000–2011 were used to drive the IBM, as described below.

2.3. Individual-Based Modelling

This study used the Hydrodynamics-based Algorithm for Lagrangian simulations (HAL; Young, 2024). This model has been used previously for simulating the transport of fish eggs, larvae and krill at both local and basin scales (Young et al., 2014, 2015, 2018, 2024; Trathan et al., 2022), and for analyses of inter-basin connectivity of *J. paulensis* populations (Silva et al., 2021). In summary, particles are advected at each model time step (5 min, chosen to ensure stability in the particle tracking scheme) according to the imposed three-dimensional velocity

field using a second-order Runge-Kutta method. Additional horizontal and vertical diffusions are included using a random-walk approach (Dyke, 2001).

The Lagrangian particles were parameterized to represent the planktonic larvae of *J. paulensis* lobsters, with specific consideration of hatching location and timing, depth distribution of larvae, and the duration of the pelagic larval stage. Particles were released at three locations at model grid cells with a depth shallower than 1,000 m: the northern island group, GI, and Vema Seamount (large-scale model only). 100 particles per grid cell per day were released during the peak hatching period from August to October, for 10 years (2000–2009), with initial particle positions randomly distributed in the horizontal and vertical (upper 100 m); over 2,000,000 particles were simulated in total. Subsequent particle transport was simulated for a total possible planktonic period of 22 months, with particles restricted to the upper 200 m of the ocean. This depth limit was guided by observations of *J. paulensis* phyllosoma larvae in the upper 200 m in the TdC region (Morley et al., 2018). Particles were reflected from both the ocean surface and the imposed depth limit to ensure they remained within the upper 200 m. There are no data describing swimming behavior or diel vertical migration (DVM) in *J. paulensis* phyllosoma larvae. However, *J. edwardsii* phyllosomas are generally regarded as having little or no directed horizontal swimming ability (Chiswell et al., 2003) and well-defined DVM has only been observed in late-stage larvae (Bradford et al., 2005). Hence, active swimming and DVM were not included in this modeling study. Successful metamorphosis to the puerulus stage and subsequent settlement was allowed from 15 months, dependent on the arrival of a phyllosoma larva in a "settlement zone" defined as model grid cells within a specified distance of one of the three source sites. Previous modeling studies of *J. edwardsii* in New Zealand assumed a settlement zone width of 100 km from the coast, following observations of the distribution of pueruli and a consideration of the swimming ability of late-stage larvae (Chiswell & Booth, 2017). However, the shelf geography of the New Zealand study region was wide and shallow, in contrast to the narrow shelves of the TdC islands, which may impact the distance from which *J. paulensis* pueruli can recruit if, for example, sound is a key orientation cue (Hinojosa et al., 2016). Therefore, for this study, three settlement zone widths were chosen for the analyses (20, 50, and 100 km) and the effect of this choice on patterns of successful larval transport was considered.

Due to limited observations of the larvae of *J. paulensis*, model parameterization choices were based on observations and prior modeling studies of *J. edwardsii* and *J. lalandii*, which have been studied in considerably more detail (Bradford et al., 2015; Pollock, 1986; Stanley et al., 2015). However, the assumed hatching and planktonic periods agree with the limited observations of *J. paulensis* phyllosoma and puerulus stages.

2.4. Analyses

The dominant transport paths of particles released from each site were calculated as the number of unique particles that passed through each model grid cell expressed as a percentage of the number of released particles; 10-year mean transport paths and the associated coefficients of variation (relative standard deviation) were visualized to qualitatively determine key persistent transport pathways for each *J. paulensis* population. Analyses were conducted for both the large-scale and regional-scale simulations, and similar plots for the subsets of particles that successfully recruited were also calculated. In addition, the 10-year mean and coefficient of variation in the locations of particles at the end of the planktonic period (22 months) was calculated for each release site to visualize particle dispersal relative to each population. The results of the large-scale simulations were further interrogated to assess the potential for basin-scale pathways for successful transport. This comprised calculation of the shortest Haversine distance between the release sites and each particle during the settlement period (15–22 months after release). These distances were binned into 100 km bins to generate histograms of particle proximity, and the median closest approach for each source and sink site was calculated. Interannual variability in total successful transport, local retention, and inter-island exchange was calculated from the 10 years of regional-scale simulations.

To further characterize the regional oceanographic environment and to investigate oceanographic drivers of successful larval transport variability, upper water column volume fluxes (upper 200 m) were calculated for a meridional (north-south) section west of the Tristan archipelago and a zonal (east-west) section located between the northern and southern island groups (Figure 2b). Mean annual cycles in fluxes were calculated and used to generate a deseasonalized time series of spatially integrated fluxes through each section. Correlations between monthly mean section fluxes and predicted successful larval transport were calculated for fluxes preceding the mean particle release month (September) by up to 8 months, and for up to 15 months after, corresponding to the

21699291, 2026, 7, Downloaded from https://agupubs.onlinelibrary.wiley.com/doi/10.1029/2025JC023603 by British Antarctic Survey, Wiley Online Library on [23/07/2026]. See the Terms and Conditions (https://onlinelibrary.wiley.com/terms-and-conditions) on Wiley Online Library for rules of use; OA articles are governed by the applicable Creative Commons License

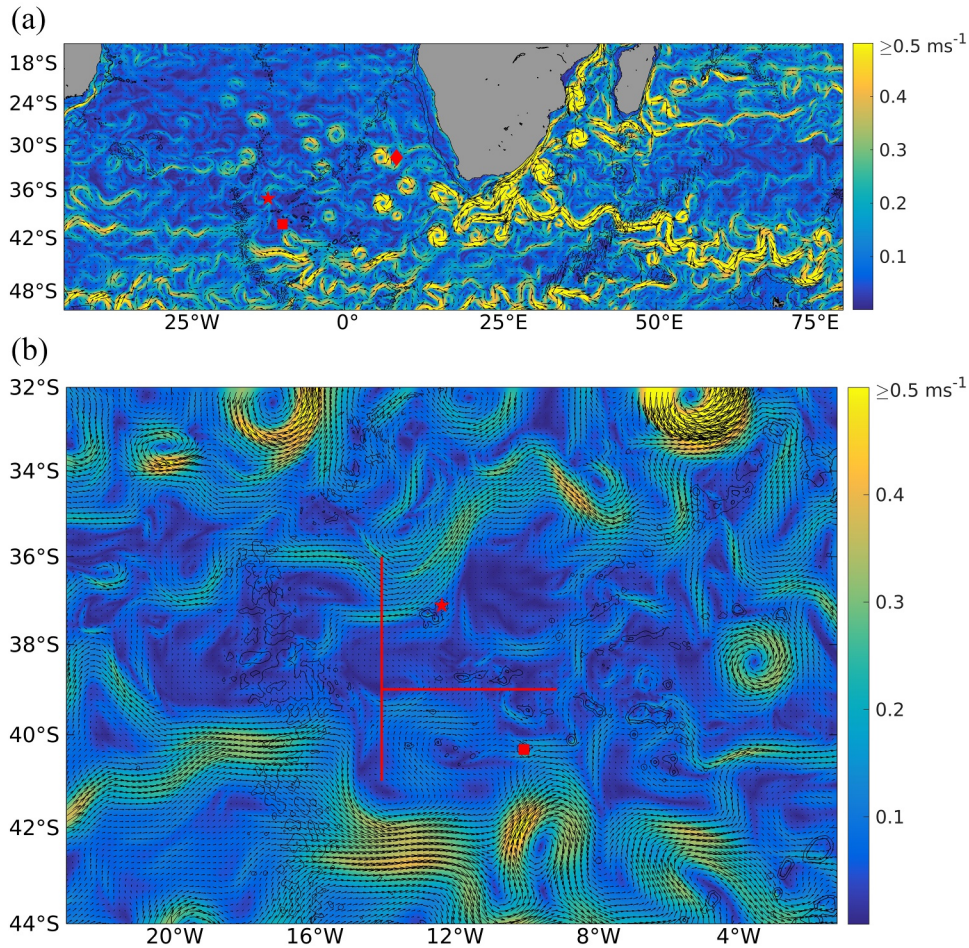

Figure 2. Simulated 10 m mean flows for September 2006 from (a) the large-scale model and (b) the regional model. Shading is current speed (m s^{-1}) and velocity vectors are plotted every (a) 10th or (b) 5th model grid cell. Key locations are marked: northern island group (star), Gough Island (square), Vema Seamount (diamond). Black contours are isobaths at 1,000 and 2,500 m. Sections used for flux analyses are shown in red (b).

start of the settlement period. Further analyses calculated correlations for fluxes averaged over periods ranging from 1 to 22 months, which encompasses the full planktonic period of the particle tracking simulations, to consider the integrative impact of oceanographic variability during the long planktonic period. The correlation between fluxes and temporal and spatial variability in wind forcing was also calculated. Longer-term impacts of climate variability were considered through correlations with the Bivariate El Nino-Southern Oscillation Index (BEST), which has been linked previously to oceanographic variability in the southwest Atlantic (Morley et al., 2025).

3. Results

3.1. Oceanographic Environment

Simulated currents from the oceanographic models capture the observed pattern of flows described previously, with broadly east to north-eastward currents in the Tristan archipelago region. In agreement with satellite data (Park & Durand, 2019), due west of the Tristan archipelago, currents associated with the southern boundary of the STFZ are deflected southward toward a persistent northward meander in the SAF and continue to the south of GI (Figure 2). Predicted flows in the southeast Atlantic region are relatively weak due to density compensation of SST gradients, and have considerable spatial and temporal variability, including multiple meanders and eddies. Of note is the representation of anticyclonic eddies around bathymetric features in the regional model (Figure 2b); such flow features likely impact dispersal and retention of marine biota (Campanella et al., 2021). The large-scale

21699291, 2026, 7, Downloaded from https://agupubs.onlinelibrary.wiley.com/doi/10.1029/2025JC023603 by British Antarctic Survey, Wiley Online Library on [23/07/2026]. See the Terms and Conditions (https://onlinelibrary.wiley.com/terms-and-conditions) on Wiley Online Library for rules of use; OA articles are governed by the applicable Creative Commons License

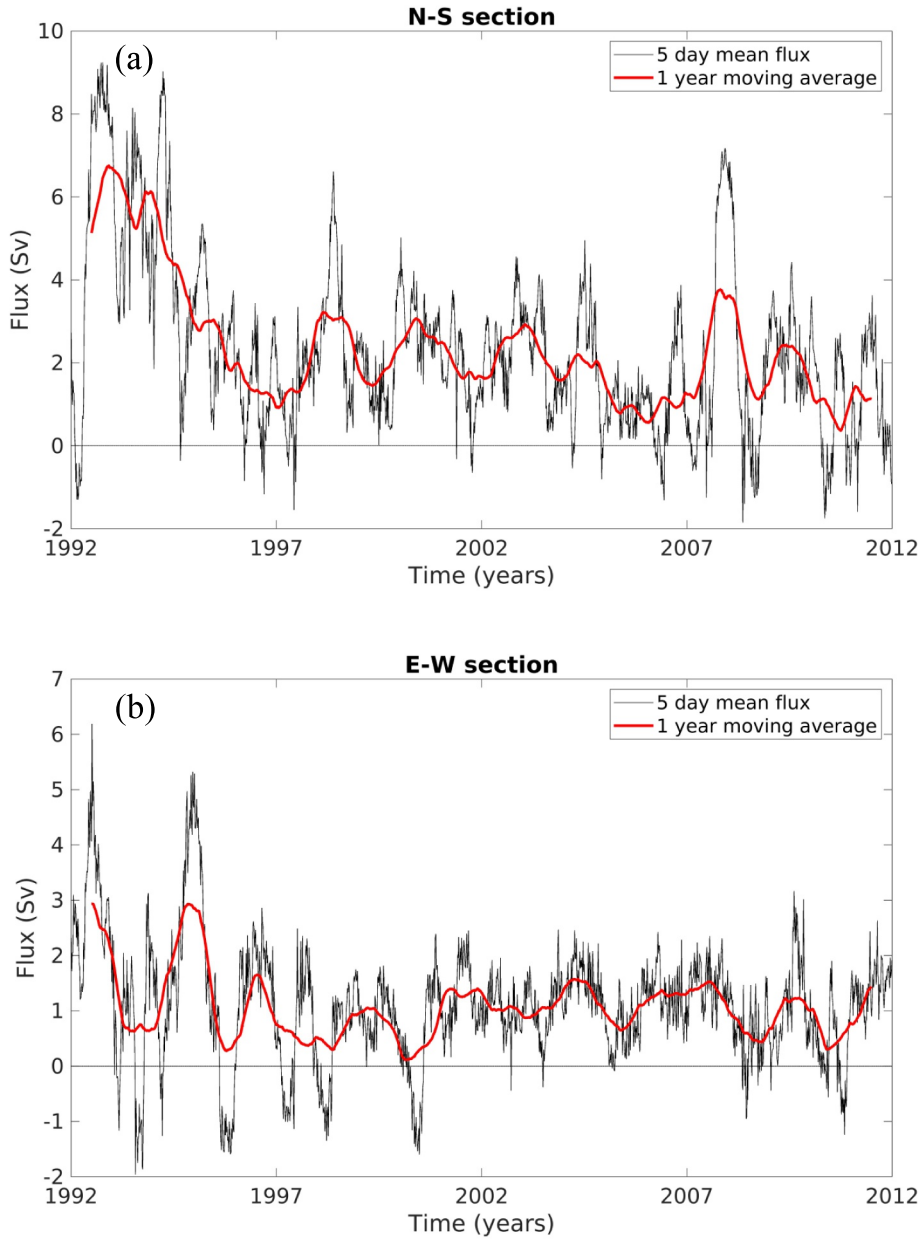

Figure 3. Time series of upper water column (<200 m depth) volume fluxes through (a) a meridional section west of the Tristan archipelago and (b) a zonal section located between the northern and southern island groups (see Figure 2).

model reproduces the Agulhas retroflection to the south of Africa. The associated eddies (Agulhas rings) traverse north-westwards across the South Atlantic and impact flows to the north and east of the Tristan archipelago (Figure 2a).

Fluxes through sections west of the Tristan archipelago and between the northern and southern island groups provide further details of variability in the regional oceanography. Considering first the 20-year (1992–2011) time series of fluxes integrated along the sections, there is a high degree of both short- and long-term variability in fluxes through both sections (Figure 3). Fluxes through the meridional (N–S) section are predominantly eastward, with mean and standard deviation in flux of 2.35 and 2.09 Sv, respectively. Fluxes through the zonal (E–W) section are predominantly northward and tend to be weaker and less variable, with mean and standard deviation in flux of 1.11 and 1.09 Sv, respectively. Deseasonalized fluxes through the meridional section are significantly positively correlated, albeit weakly, with fluxes through the zonal section, with strongest correlations for fluxes

21699291, 2026, 7, Downloaded from https://agupubs.onlinelibrary.wiley.com/doi/10.1029/2025JC023603 by British Antarctic Survey, Wiley Online Library on [23/07/2026]. See the Terms and Conditions (https://onlinelibrary.wiley.com/terms-and-conditions) on Wiley Online Library for rules of use; OA articles are governed by the applicable Creative Commons License

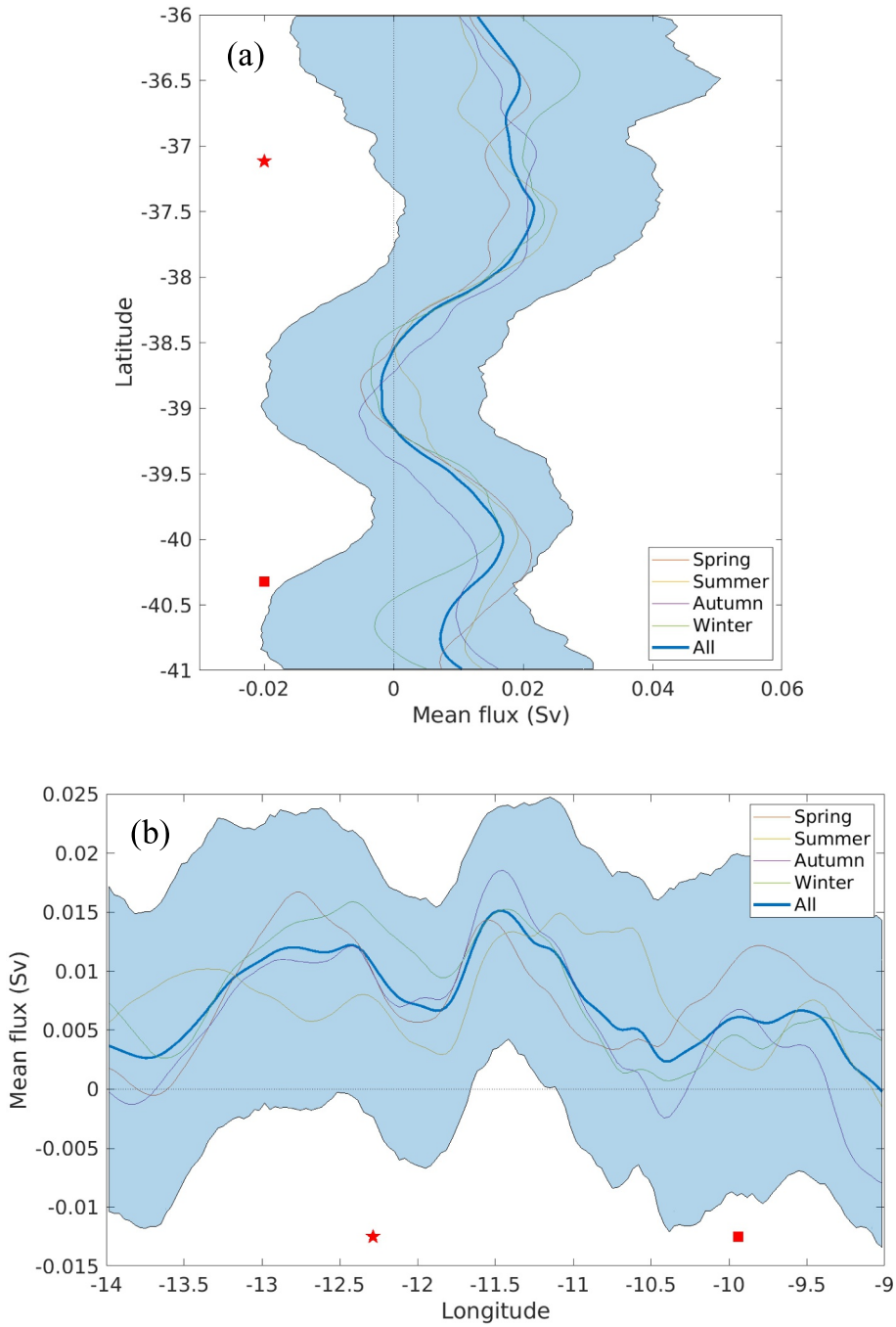

Figure 4. Twenty-year mean upper water column fluxes with shading between the 0.25 and 0.75 quantile ranges and mean seasonal fluxes through (a) a meridional section west of the Tristan archipelago and (b) a zonal section located between the northern and southern island groups (see Figure 2). For reference, the latitude and longitude of the northern islands (red stars) and Gough Island (red squares) are shown.

through the zonal section 65 days earlier ($r = 0.1918$, $p < 0.001$). The mean seasonal cycles of normalized fluxes through the sections exhibit similar patterns and are more strongly correlated ($r = 0.5093$, $p < 0.001$). The seasonality in fluxes is particularly clear for the meridional section with weaker fluxes in early autumn and early spring (not shown).

Resolving the spatial structure of fluxes through the sections, the time-mean flux through the meridional section suggests two regions of strongest flows (Figure 4a). The first peak, at approximately 40°S, is associated with the

21699291, 2026, 7, Downloaded from https://agupubs.onlinelibrary.wiley.com/doi/10.1029/2025JC023603 by British Antarctic Survey, Wiley Online Library on [23/07/2026]. See the Terms and Conditions (https://onlinelibrary.wiley.com/terms-and-conditions) on Wiley Online Library for rules of use; OA articles are governed by the applicable Creative Commons License

21699291, 2026, 7, Downloaded from https://agupubs.onlinelibrary.wiley.com/doi/10.1029/2025JC023603 by British Antarctic Survey, Wiley Online Library on [23/07/2026]. See the Terms and Conditions (https://onlinelibrary.wiley.com/terms-and-conditions) on Wiley Online Library for rules of use; OA articles are governed by the applicable Creative Commons License

SSTF, and lies at approximately the latitude of GI. There is little seasonal variability in the location of the SSTF at this longitude; peak fluxes are located slightly further south in spring and autumn (40.2°S) relative to summer and winter (40°S). There is a broad peak in fluxes between approximately 38°S and 36°S, associated with the Tristan Current (Vianna & Menezes, 2011) and lying at approximately the latitude of the northern island group. This exhibits more seasonal variability than the peak to the south and there is a suggestion of multiple peaks, with strongest fluxes at 37.5°S in summer and at 36.5°S in winter. Mean fluxes through the zonal section are generally weaker and more variable than fluxes through the meridional section (Figure 4b). Broadly, northward fluxes are dominant, but the 0.25 quantile suggests frequent southward fluxes, with preferred locations for southward flow centered at 13.75°W, 10.5°W, and 9°W.

The role of regional winds in driving oceanographic variability was examined by calculating correlations between the 20-year time series of fluxes integrated along the sections (Figure 3) and the reanalysis winds used as atmospheric forcing for the regional model. Reanalysis winds were temporally averaged to the same 5-day means as the oceanographic fluxes and spatially averaged over the regional model domain. Lead-lag correlations were calculated for eastward and northward components of wind preceding the 5-day mean flux by up to 6 months. Focusing on fluxes through the upper 200 m, fluxes through the meridional section (positive eastward) are negatively correlated with northward winds, with the strongest correlation for zero temporal offset ($r = -0.23$; $p < 0.001$). Fluxes through the zonal section (positive northward) are positively correlated with eastward winds, with the strongest correlation for zero temporal offset ($r = 0.28$; $p < 0.001$). There was also a significant positive correlation between eastward winds and fluxes through the meridional section, which was also apparent in correlations with the full-depth fluxes. Correlations were significant for winds preceding fluxes by ~4.5–6 months, with the strongest correlation for winds preceding upper 200 m fluxes by ~5.5 months ($r = 0.1151$; $p < 0.001$).

Impacts of climate variability on regional winds and hence oceanographic variability were considered through correlations of monthly averaged reanalysis winds (ERA5) with the Bivariate El Nino-Southern Oscillation Index (BEST) using the available overlapping 83-year time period (1940–2022). Correlations were calculated for BEST preceding the eastward and northward components of wind by up to 4 years. There was a significant positive correlation between BEST and eastward regional winds, with the strongest correlation for BEST preceding winds by 1 month ($r = 0.1402$; $p < 0.001$). The spatial pattern of correlations showed significant positive correlations ($p < 0.001$) between BEST and eastward winds for most of the regional model domain, excluding the southeast corner (Figure S5 in Supporting Information S1). Thus, during El Niño events (positive BEST), there is a tendency for stronger eastward winds in the TdC region.

3.2. Large-Scale Transport

The large-scale particle simulations reveal a dominant east-north-eastward transport of particles from the Tristan archipelago, as illustrated by the 10-year mean and coefficient of variation in predicted pathways (Figures 5a–5d). The west-east bands of low coefficient of variation suggest a persistent transport pathway eastward to the Indian Ocean for particles released at the Tristan archipelago (Figures 5b and 5d), particularly for GI. Particles released at the Vema Seamount follow a broad west or north-westward pathway (Figures 5e and 5f).

After 22 months, particles released at all three sites are widely dispersed (Figure 6). For particles released at the northern island group, the highest concentration is persistently located in the southeast Atlantic Ocean (Figures 6a and 6b). The distribution of particles extends from ~35°W to the model limit at 80°E, but the high coefficient of variation at the extremes of the distribution highlights the intermittent nature of such transport. For particles released at GI, the distribution pattern extending east into the Indian Ocean is more persistent (Figures 6c and 6d), which supports observations of genetic connectivity between *J. paulensis* populations in the Atlantic and Indian Oceans (Silva et al., 2021). However, the highest concentration of particles is again located in the southeast Atlantic Ocean (Figure 6c). Particles released at Vema Seamount spread further to the northwest than those released at the other two locations, and unlike particles released at the Tristan archipelago, few particles are found close to the latter islands after 22 months (Figure 6e).

To further clarify the potential for successful basin-scale transport, histograms of the proximity of particles to each of the three release sites during the settlement period were generated and the median closest approach for each source and sink site was calculated (Figure S6 in Supporting Information S1). The results suggest that for all release sites the majority (>84%) of particles are not transported within 100 km of any site during the settlement

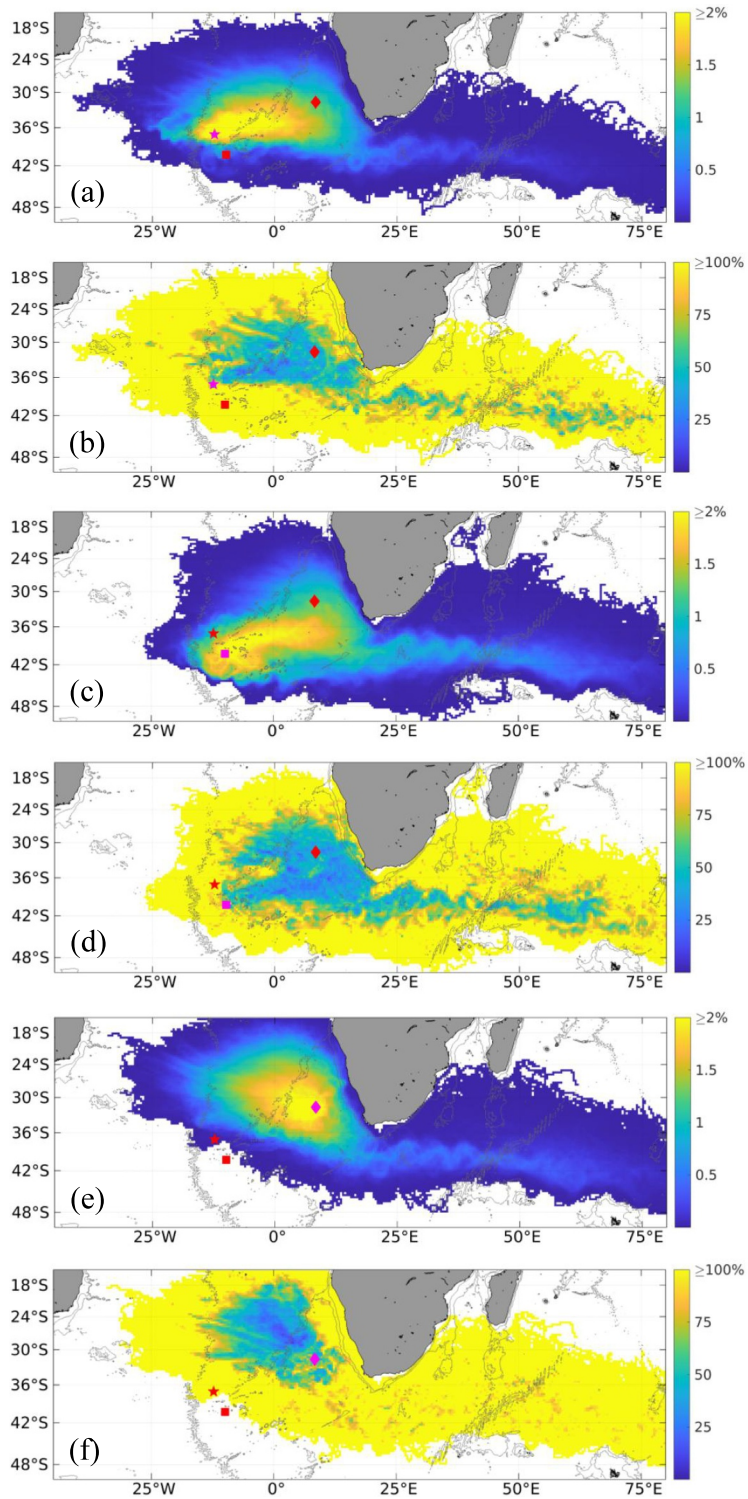

Figure 5. Predicted 10-year mean pathways (a, c, e) and coefficient of variation (b, d, f) for particle releases at (a, b) the northern island group, (c, d) Gough Island (GI), and (e, f) Vema Seamount. Values are integrated onto a grid 5× coarser than the underlying model grid. Mean pathways are plotted as log transformed percentages ($\log(10x + 1)$) to better visualize the distributions. Key locations are marked: the northern island group (star), GI (square), Vema Seamount (diamond). The marker of the relevant particle release location is colored magenta.

21699291, 2026, 7, Downloaded from https://agupubs.onlinelibrary.wiley.com/doi/10.1029/2025JC023603 by British Antarctic Survey, Wiley Online Library on [23/07/2026]. See the Terms and Conditions (https://onlinelibrary.wiley.com/terms-and-conditions) on Wiley Online Library for rules of use; OA articles are governed by the applicable Creative Commons License

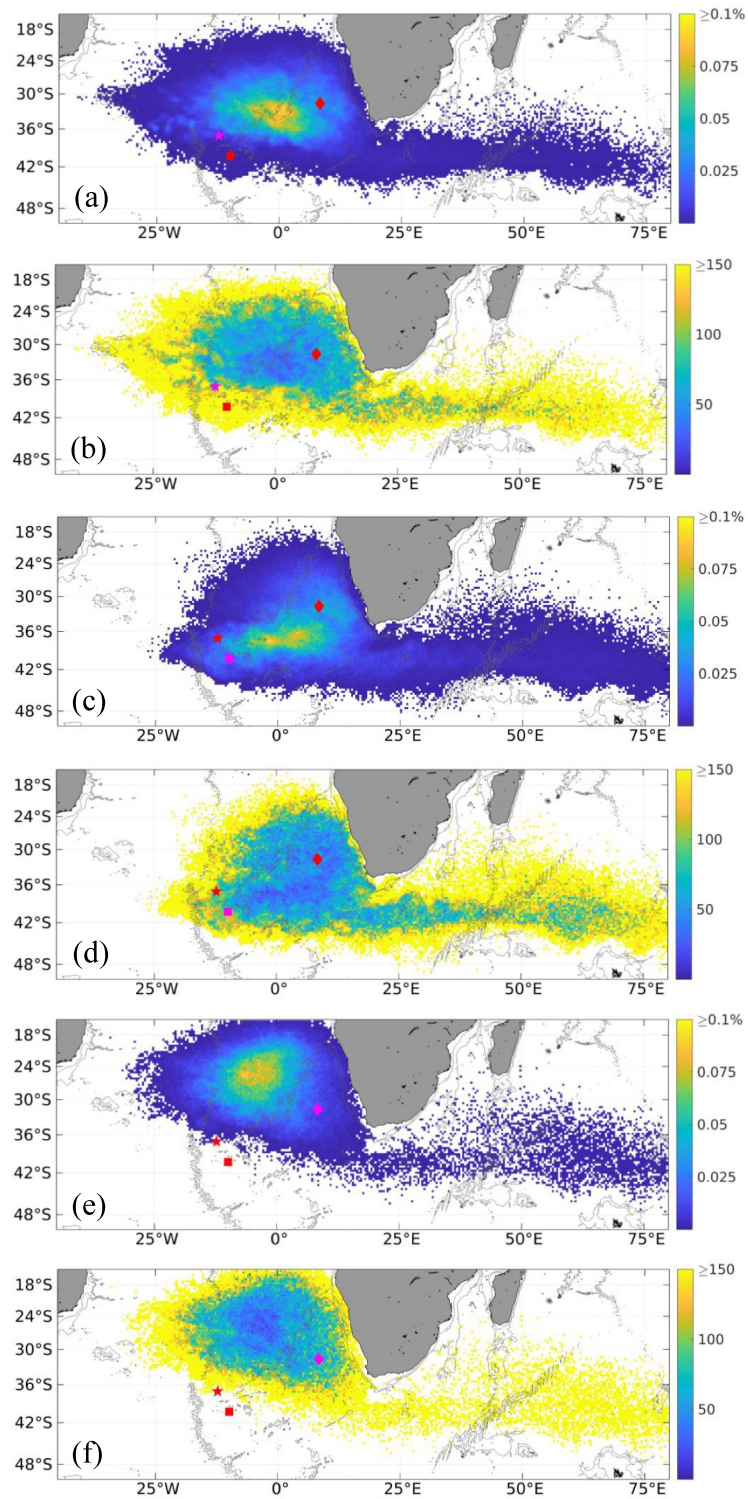

Figure 6. Predicted 10-year mean particle distribution as a percentage of the number of particles released at each location (a, c, e) and coefficient of variation (b, d, f) after 22 months for releases at (a, b) the northern island group, (c, d) Gough Island (GI), and (e, f) Vema Seamount. Values are integrated onto a grid 5× coarser than the underlying model grid. Key locations are marked: the northern island group (star), GI (square), Vema Seamount (diamond). The marker of the relevant particle release location is colored magenta.

21699291, 2026, 7, Downloaded from https://agupubs.onlinelibrary.wiley.com/doi/10.1029/2025JC023603 by British Antarctic Survey, Wiley Online Library on [23/07/2026]. See the Terms and Conditions (https://onlinelibrary.wiley.com/terms-and-conditions) on Wiley Online Library for rules of use; OA articles are governed by the applicable Creative Commons License

21699291, 2026, 7, Downloaded from https://agupubs.onlinelibrary.wiley.com/doi/10.1029/2025JC023603 by British Antarctic Survey, Wiley Online Library on [23/07/2026]. See the Terms and Conditions (https://onlinelibrary.wiley.com/terms-and-conditions) on Wiley Online Library for rules of use; OA articles are governed by the applicable Creative Commons License

Table 1
Ten-Year Mean and Standard Deviation (in Brackets) in Percentage of Particles Released at Source Sites (Northern Island Group and Gough Island) Successfully Reaching Either Destination Within the Larval Settlement Period for Settlement Zones of 100 and 20 km

		Destination			
		Northern island group		Gough Island	
		100 km	20 km	100 km	20 km
Source	**Northern island group**	4.6 (3.8)	1.8 (2.1)	0.7 (0.8)	0.1 (0.2)
	Gough Island	7.5 (4.6)	2.5 (1.6)	4.4 (3.1)	0.7 (0.9)

period and are unlikely to settle successfully. The percentages of particles released at the northern islands and GI that successfully reach Vema Seamount (7.5% and 7.6%, respectively) exceed the percentage retained at Vema Seamount (4.6%), which highlights the importance of upstream sources of larvae for settlement at this location. By contrast, no particles released at Vema Seamount reach GI during the settlement period, and only 0.02% reach the northern islands. Thus, while settlement at Vema Seamount is enhanced by large-scale transport from upstream sources, settlement at the northern islands and GI depends on local retention and regional-scale transport between the islands. The model results indicate that an anticyclonic pathway for successful transport via a complete circuit of the South Atlantic Gyre is not feasible over a 22-month planktonic phase, confirming the assessment of Glass (2014).

The particle distributions after 22 months (Figure 6) and analyses of particle proximity to release sites show that a small percentage of particles released at islands of the Tristan archipelago are retained close to the islands. This retained percentage is highly variable and is sensitive to the representation of mesoscale current features in the

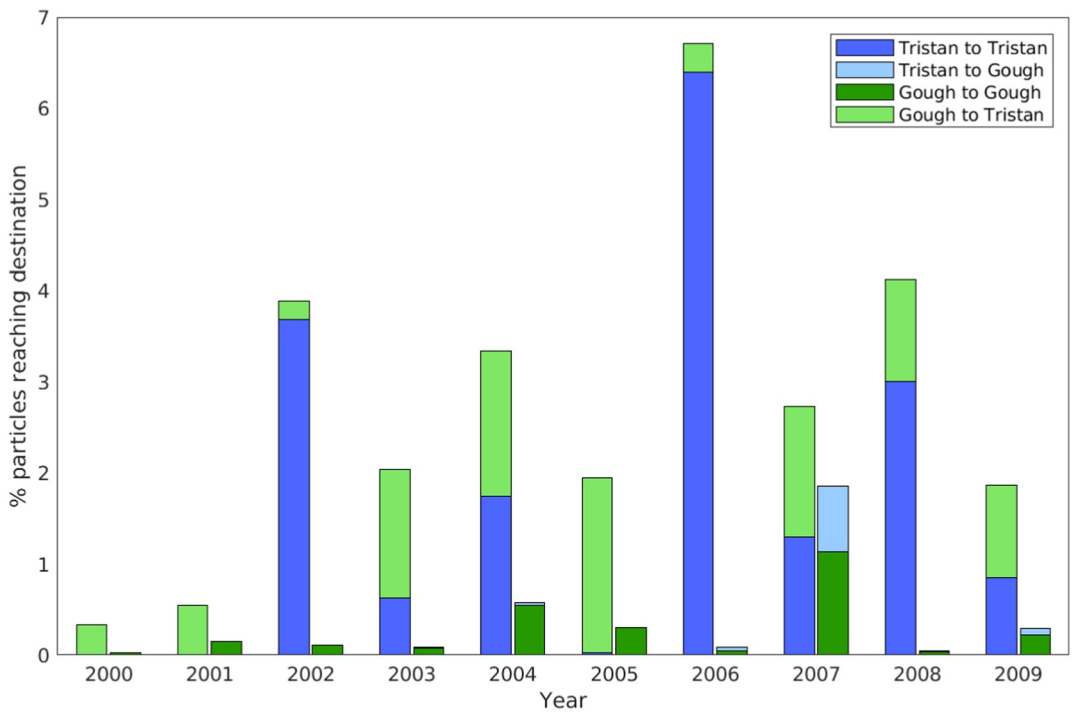

Figure 7. Simulated inter-annual variability in successful transport from the high-resolution model; bars show successful particle transport to each location by source as a percentage of the total number of particles released, with left-hand bars corresponding to transport to the northern island group and right-hand bars corresponding to Gough Island (GI). Retention at the natal site for the northern island group and GI are dark blue and dark green, respectively. Transport from GI to the northern island group and vice versa are shaded light green and light blue, respectively.

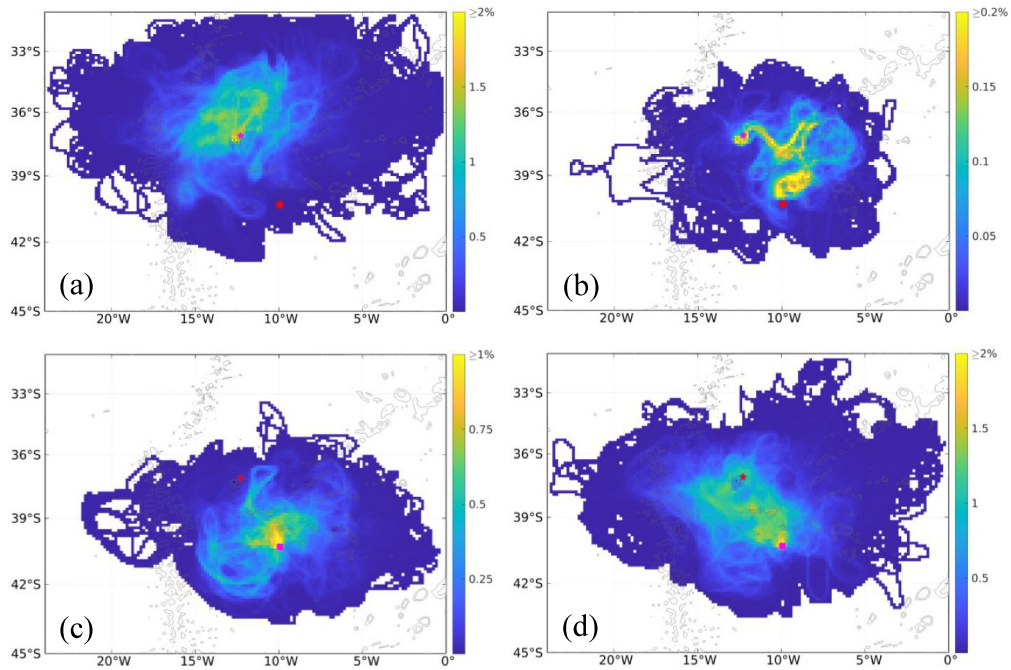

Figure 8. Predicted 10-year mean pathways for particle releases at (a, b) the northern island group, and (c, d) Gough Island (GI). Retention for the northern island group and GI is shown in (a) and (c), respectively. Exports from the northern islands to GI are shown in (b) and from GI to the northern islands in (d). Pathways are integrated onto a grid 5× coarser than the underlying model grid and are plotted as log transformed percentages ($\log(10x + 1)$) to better visualize the distributions. Key locations are marked: the northern island group (star) and GI (square). The relevant particle release location is colored magenta.

model. The high-resolution model is better able to resolve such features, thus analyses of inter-island transport and retention focus on the results of particle tracking simulations with the regional model.

3.3. Regional-Scale Transport and Retention

Considering first the 10-year mean retention and inter-island exchange (Table 1), the model suggests that, on average, a higher percentage of particles released at GI is successfully transported to the northern island group than is locally retained, regardless of the size of settlement zone. Conversely, GI receives few larvae from the northern island group, which suggests that the lobster stock at GI is dependent on the retention of locally produced larvae. Simulated successful transport shows a high degree of inter-annual variability (Figure 7). Retention and inter-island exchange are reduced for both sites if a smaller settlement zone is used in the analysis, but the overall patterns in variability are broadly similar; thus, the remainder of this section focuses on the results with a 20 km settlement zone. In 2000, 2001, and 2005, there is negligible retention of larvae in the northern island group (<0.03%) and settlement in these years relies on imports from GI. Further, there are only four years in which the percentage of retained larvae at the northern island group exceeds that imported from GI (2002, 2004, 2006, 2008), which emphasizes the importance of GI as a source of larvae for the lobster population at the northern island group. Transport from the northern island group to GI is negligible in all years except 2007, and even in 2007, the contribution of retention at GI to overall settlement is more important. The maintenance of the lobster population at GI thus depends on the retention of larvae. The total settlement at GI is always lower than that at the northern island group (Figure 7); the GI population may therefore be more sensitive to biotic and abiotic pressures.

Statistical analyses of the time series reveal a positive but non-significant correlation between retention at GI and exports to the northern island group ($r = 0.51$; $p = 0.13$), and a negative non-significant correlation between retention at the northern island group and imports from GI ($r = -0.43$; $p = 0.22$). Although non-significant, the latter suggests a level of reliability in settlement at the northern island group; settlement in years with poor

21699291, 2026, 7, Downloaded from https://agupubs.onlinelibrary.wiley.com/doi/10.1029/2025JC023603 by British Antarctic Survey, Wiley Online Library on [23/07/2026]. See the Terms and Conditions (https://onlinelibrary.wiley.com/terms-and-conditions) on Wiley Online Library for rules of use; OA articles are governed by the applicable Creative Commons License

21699291, 2026, 7, Downloaded from https://agupubs.onlinelibrary.wiley.com/doi/10.1029/2025JC023603 by British Antarctic Survey, Wiley Online Library on [23/07/2026]. See the Terms and Conditions (https://onlinelibrary.wiley.com/terms-and-conditions) on Wiley Online Library for rules of use; OA articles are governed by the applicable Creative Commons License

retention is augmented by imports of larvae from GI (e.g., 2003 and 2005), although the model suggests there are still years when overall settlement is poor (e.g., 2000 and 2001).

The 10-year mean transport pathways for particles retained at the northern island group and GI, or exported between these locations, suggest that some particles can be transported considerable distances away from the archipelago before successfully returning to settle (Figure 8). The complex oceanography of the region, including bathymetrically driven circulation features, retains particles in eddies and current meanders, which facilitates transport against the prevailing east to north-eastward flows during the extended planktonic larval phase. Transport paths for particles retained in the northern island group are concentrated in a region extending west to northeast of the islands (Figure 8a). Paths for particles retained at GI are concentrated in a broad region to the north of the island, with a further notable pathway extending in a loop to the southwest (Figure 8c). Exports from the northern island group to GI mainly occurred in a single simulation year (2007; Figure 7), so variability in transport paths for this subset is reduced. Most particles are transported eastwards, becoming retained in eddies before being transported south or southwest to GI (Figure 8b). Particles exported from GI to the northern island group follow a predominantly north-westward route, with a significant percentage approaching the northern island group from the southwest (Figure 8d).

3.4. Oceanographic Drivers of Larval Transport Variability

To explore oceanographic influences on the variability in successful regional transport, correlations between annual retention and export and monthly mean fluxes through the meridional and zonal sections described earlier (Section 3.1; Figure 2) were calculated, as detailed in Section 2.4. The results described here focus on fluxes through the upper 200 m, which are of most relevance to the transport of lobster larvae, although full-depth fluxes are also considered. Correlations are presented for p-values less than 0.01 and 0.05. A compilation of key results is included here; all significant correlations are shown in Tables S2–S5 in Supporting Information S1. In the following description, fluxes through the meridional section are positive eastward and fluxes through the zonal section are positive northward; references to "weaker" flux can be either a weakening or a reversal of the flow.

First considering successful transport to the northern island group, weaker eastward fluxes through the upstream meridional section about 4–6 months before peak September hatching support stronger retention at the northern island group. Stronger northward fluxes through the zonal section about 1 yr after peak September hatching and averaged for 2–4 months also support stronger retention at the northern island group, as do stronger eastward flows through the meridional section over similar time periods. For the latter, as there is a positive correlation between fluxes through the two sections (Section 3.1), it is unclear if the underlying driver of higher retention is increased eastward or northward fluxes or both. Increased export from GI to the northern islands is associated with weaker long-term (17-month average) fluxes through the meridional section from about 6 months after peak September hatching. The increased export from GI and decreased retention at the northern islands associated with weaker eastward fluxes in the months before the settlement period may be the underlying mechanism behind the negative relationship between these settlement measures noted in Section 3.3. Although not significant, with a p-value >0.05, there is a suggestion that stronger northward fluxes through the zonal section about 4 months after peak September hatching support increased export from GI to the northern islands.

Stronger retention at GI is associated with weaker eastward fluxes through the upstream meridional section for averaging periods of 3–7 months starting 7–10 months after peak September hatching. Thus, weaker eastward fluxes over long time periods support both increased retention at GI and increased export to the northern islands, which may be the underlying mechanism for the positive relationship between these measures noted in Section 3.3. Weaker northward fluxes through the zonal section over a sustained period of 10 months for 9 months after peak September hatching also support stronger retention at GI. The analyses suggest that these weaker fluxes also support stronger exports from the northern islands to GI. However, there is only one year with notable exports (2007; Figure 7), so this correlation is questionable. Similarly, the correlation between increased export from the northern islands to GI and stronger eastward fluxes through the meridional section during the approximately 4-month period after peak hatching should be interpreted with caution. A comparison of the time series of successful transport (Figure 7) with the time series of fluxes through the meridional section (Figure 3a) suggests that the high export following hatching in 2007 may be due to an anomalously strong flux through the meridional section in late 2007 to early 2008. However, there are other periods of strong flux through the meridional section that do not drive similar pulses of increased settlement. Therefore, this is a potentially anomalous event with unusually strong

21699291, 2026, 7, Downloaded from https://agupubs.onlinelibrary.wiley.com/doi/10.1029/2025JC023603 by British Antarctic Survey, Wiley Online Library on [23/07/2026]. See the Terms and Conditions (https://onlinelibrary.wiley.com/terms-and-conditions) on Wiley Online Library for rules of use; OA articles are governed by the applicable Creative Commons License

fluxes during a key period of the planktonic phase; future studies could consider extending the number of years used in hindcasts to evaluate the rarity of such settlement pulses. Variability in successful larval transport is of course driven by more than just variability in oceanographic fluxes, which can be thought of as constraining the proportion of larval production arriving at a given location, independent of factors affecting the number of larvae produced or their survival during dispersal, such as SST. A more accurate reflection of larval dispersal would be inclusive of environmental conditions relative to the thermal niche of the species and adjust predictions of cohort recruitment strength accordingly.

4. Discussion and Conclusions

Effective management of the Tristan rock lobster (*J. paulensis*) fishery in the remote archipelago of TdC can be enhanced by an understanding of environmental factors impacting stock recruitment. In this study, we have focussed on the role of oceanographic variability, specifically ocean currents, in larval transport variability, including a consideration of large-scale connectivity to investigate the potential role of upstream sources in the supply of larvae to the TdC archipelago.

At the basin-scale, no particles released at Vema Seamount reached GI during the settlement period, and only 0.02% reached the northern islands, which suggests that historical populations of *J. paulensis* at Vema Seamount did not support populations at the Tristan archipelago. Following intensive commercial exploitation at Vema Seamount in the 1960s, the population decreased dramatically and has not shown consistent signs of recovery (Von Der Heyden et al., 2007). This is perhaps surprising given the consistent transport to Vema Seamount from both GI and the northern island group suggested by basin-scale simulations; successful transport was predicted in all 10 years with mean transports of 7.5% and 7.6% for the northern island group and GI, respectively. However, phyllosoma larvae are only able to metamorphose into the puerulus settling stage when they encounter specific physical and/or chemical cues similar to their natal environments (Pollock, 1990). It is possible that too few lobsters remain on the seamount to provide settling cues for new recruits (Von Der Heyden et al., 2007). Model simulations revealed a persistent transport pathway eastward to the Indian Ocean for particles released at the Tristan archipelago, particularly from GI, which supports observations of genetic connectivity between *J. paulensis* populations in the Atlantic and Indian Oceans (Silva et al., 2021). However, simulations by Silva et al. (2021) found no direct westward transport from islands of the Indian Ocean to the Tristan archipelago; thus, Indian Ocean *J. paulensis* populations are unlikely to act as sources for populations at the Tristan archipelago in the present oceanographic regime. Basin-scale simulations also suggested that transport to the Tristan archipelago via a complete circuit of the South Atlantic Gyre, previously suggested by Pollock (1991), is not feasible within the time frame of the planktonic larval phase. Thus, larval settlement at the northern islands and GI likely depends on local retention and regional-scale transport pathways.

Regional modeling suggested a high degree of temporal variability in both retention at the northern island group and GI, and inter-island exchange. Transport from the northern island group to GI was sporadic, with significant transport in only one of the 10 simulation years (2007). However, there was transport from GI to the northern island group predicted in all simulation years, with a mean particle export of 2.5% for a 20 km settlement distance. This regular export of larvae supports observations of a lack of genetic differentiation between the two populations (Silva et al., 2021; Von Der Heyden et al., 2007). The predominantly one-way inter-island exchange has implications for the management of the lobster populations at GI and the northern island group. At GI, with weak, sporadic imports from the northern island group, the local population is strongly dependent on successful retention. Further, as overall successful larval transport to GI is always lower than that at the northern island group, the GI population may be more sensitive to biotic pressures such as viruses (Danovaro et al., 2011), parasites (Byers, 2021), and competition from invasive species, such as the invasive South American silver porgy (*Diplodus argenteus*), which is spreading around the northern islands (Caselle et al., 2017). The same will likely be true for abiotic pressures, such as increases in ocean temperatures (Garcia-Soto et al., 2021) and shifts in ocean currents (Wilson et al., 2016) due to ongoing climate change. The lobster population at GI therefore requires careful management to ensure it remains sustainable in the long term. The population in the northern island group is less susceptible to short-term biotic or environmental pressures as the combination of larval retention and imports from GI ensures a strong supply of recruits in most years.

Comparisons of simulated successful larval transport with regional oceanographic fluxes revealed the role of ocean currents in the interannual variability of retention and inter-island exchange. A mean strengthening of

21699291, 2026, 7, Downloaded from https://agupubs.onlinelibrary.wiley.com/doi/10.1029/2025JC023603 by British Antarctic Survey, Wiley Online Library on [23/07/2026]. See the Terms and Conditions (https://onlinelibrary.wiley.com/terms-and-conditions) on Wiley Online Library for rules of use; OA articles are governed by the applicable Creative Commons License

eastward flows during the planktonic period was associated with lower retention at GI, and a reduction in export of larvae to the northern island group. Similarly, stronger eastward flows in the months prior to peak hatching were associated with weaker retention in the northern island group. By contrast, stronger eastward flows during the months before the start of the settlement period were associated with stronger successful transport to the northern island group, although the underlying mechanism is unclear due to a related coincident strengthening in northward fluxes. Stronger mean northward fluxes during the latter half of the planktonic period were also associated with weaker retention at GI. Model analyses suggested that stronger eastward flows and weaker northward flows increased the export of larvae from the northern island group to GI. However, this result is based on a single year of notable export with anomalously high eastward flows a few months after peak hatching; therefore, a degree of caution in interpretation is required.

Variability in oceanographic flows is strongly influenced by regional wind forcing, in particular through Ekman dynamics whereby winds generate a net movement of water within the Ekman layer (typically of the order 100 m) 90° to the left of the wind direction, as well as influencing rates of vertical transport. Thus, analysis of fluxes through zonal and meridional sections suggests that stronger westerly winds drive an increase in northward flows and stronger northerly winds drive an increase in eastward flows. There is also a delayed oceanographic response to westerly winds, weaker than the direct response of upper ocean flows through Ekman transport, whereby wind-driven steepening of sea surface height gradients across the southern limb of the SASG results in a barotropic (full-depth) increase in eastward flows. Variability in the regional winds is related to large-scale climate variability; there is a positive correlation between BEST and westerly regional winds and the spatial pattern of correlations showed significant positive correlations for most of the TdC region. Thus, during El Niño events there is a tendency for stronger westerly winds in the TdC region.

The links demonstrated here between climate variability, winds, oceanographic flows, and larval transport have implications for the response of lobster populations to future climate change. A study of the impact of climate change on the dispersal and survival of *Sagmariasus verreauxi* (eastern rock lobster) larvae in south-eastern Australia found that while warmer ocean temperatures favored larval survival, changes in ocean currents altered dispersal patterns and negatively impacted the supply of larvae to coastal settlement sites (Cetina-Heredia et al., 2015). High-resolution climate models consistently project a future intensification and southward shift of the Southern Hemisphere westerlies, leading to a southward migration of the SSTF, expansion of subtropical gyres, and strengthening of the SASG, particularly at its southern boundary (Graham et al., 2012; Marcello et al., 2023). These shifts are attributed to changes in wind patterns, a more positive Southern Annular Mode (SAM), and increased near-surface warming that enhances vertical stratification of the water column (Peng et al., 2022). While ensemble simulations suggest complex but generally eastward flow increases in the TdC region, observational data from 1993 to 2018 show a significant southward migration of the southern boundary of the SASG but no clear trends in gyre size or strength (Drouin et al., 2021). Yang et al. (2020) similarly noted a small poleward gyre displacement linked to shifting wind fields. Regional studies of the South Atlantic showed correlations between El Niño Southern Oscillation (ENSO), SST, and productivity, the latter an indicator of food availability during the larval period (Ford et al., 2021; Morley et al., 2025) largely driven by increased westerly winds and an associated increase in surface mixing, suggesting that wind-driven changes and stratification impact the regional ecosystem. El Niño events are expected to become more frequent and extreme with climate change (Cai et al., 2014; Wang et al., 2017) and SAM is expected to be more frequently in a high index state (Fogt & Marshall, 2020) with consequent impacts on wind fields. However, a degree of caution is required when considering future projections of ENSO variability due to inter-model spread in climate model forecasts (Chung et al., 2024) and biases in their representation of historical ENSO variability (Erickson & Patricola, 2023). Regardless, this study has shown that such changes are likely to affect lobster larval transport, retention, and settlement around the TdC archipelago.

The body temperature of ectotherms varies with water temperature; therefore, warming oceans will have strong biological effects on the rates of all physiological functions of lobster larvae (Hochachka & Somero, 2002). Within their thermal tolerance window, increases in temperature are expected to increase growth and development rates. In the congeneric lobster *J. edwardsii*, the growth rate was highest at 18.2°C but was reduced again at 21.5°C when high mortality was also observed (Bermudes & Ritar, 2008). The thermal window for *J. paulensis* is unknown but, as demonstrated by this study, implications for larval survival and growth will likely be complex, with subsequent impacts on ecological fitness also anticipated (e.g., Twiname et al., 2022). Several studies have demonstrated that crustacean larval mortality is increased by changes in SST (e.g., Deschamps et al., 2025;

21699291, 2026, 7, Downloaded from https://agupubs.onlinelibrary.wiley.com/doi/10.1029/2025JC023603 by British Antarctic Survey, Wiley Online Library on [23/07/2026]. See the Terms and Conditions (https://onlinelibrary.wiley.com/terms-and-conditions) on Wiley Online Library for rules of use; OA articles are governed by the applicable Creative Commons License

Hobday & Pecl, 2014; Marochi et al., 2022; Monteiro et al., 2023). Climate change will not affect *J. paulensis* in isolation but will have cascading effects throughout the ecosystem. This is particularly important because *J. paulensis* lives in shallow water kelp forests, which are known to be highly sensitive to warming (Smale et al., 2019). Fortunately, around the TdC archipelago, the main habitat-forming species (giant kelp, *Macrocystis pyrifera*) seems to have a low risk of climate-induced range shifts in this century, with the notable caveat that kelp forests are vulnerable to marine heatwaves and it remains highly uncertain how their incidence and intensity will change under different climate change scenarios (Engelhard et al., submitted).

This study has focussed on the role of oceanographic variability in *J. paulensis* larval transport and settlement. However, in the context of fisheries management, there are a number of further considerations required. With regard to the regional oceanographic model, although there is a good representation of mesoscale variability, including the interaction of oceanographic flows with complex bathymetry, the grid is not sufficiently fine to fully resolve channels between the islands of the northern island group or complex fine-scale oceanography due to headlands or small bays. Such small-scale oceanographic features may enhance local retention around the islands (Morgan et al., 2011) and increase rates of returning larvae to the northern island group, reducing the dependence on imports of larvae from GI. The early life history of *J. paulensis* is not well known and there is therefore uncertainty in the choice of model parameterization, such as the length of the planktonic phase and larval behavior, which adds uncertainty to the interpretation of the model simulations. This modeling study also does not include important biological influences on fisheries recruitment such as variable spawning stock biomass and fecundity, larval mortality, or post-settlement survival, which complicates interpretation of the model output with regard to population variability and fisheries management. For example, higher post-settlement survival rates at Inaccessible Island compared to Nightingale Island in the northern island group are likely related to differences in the island topographies (Pollock, 1991). Whilst the subtidal zone generally drops off abruptly at Nightingale Island, Inaccessible Island has a more gently sloping subtidal region with a multitude of rocks and boulders to provide shelter and refuge from predatory fish. Recent scientific research cruises to the region (JR17-004 (Morley et al., 2018) and DY100 (Whomersley et al., 2019)) observed *J. paulensis* puerulus and large phyllosoma larvae in proximity to the Tristan archipelago, while analyses of historical catches suggest only smaller phyllosoma larvae across the wider South Atlantic (Pollock, 1991). This suggests that only larvae entrained in regional transport pathways or in small-scale local retention features successfully grow, develop and recruit to *J. paulensis* populations at TdC. Phyllosoma larvae transported more widely may be subject to lower and more patchy food availability (Campanella et al., 2021) with subsequent lower growth and higher mortality.

The models used in this study have estimated a large variability in retainment of larvae, with particularly high larval retention at TdC for larvae hatched in 2002 and 2006. *J. paulensis* recruit to the fishery at around 5 years old (3–7 years old; Booth, 2006); therefore, if oceanographic variability was the primary driver of recruitment variability, peaks in settlement would be expected to translate into increased fishery recruitment in 2007 and 2011. There was a strong peak in catch per unit effort (CPUE) at TdC in 2007. However, there was only a marginally elevated CPUE in 2011, although this was followed by a number of years of reduced CPUE (Johnston, 2025). Thus, while this study has shown that oceanographic variability can have a strong influence on the transport and retention of *J. paulensis* larvae in the South Atlantic, there are a multitude of other environmental and biological factors, such as the impact of increasing ocean temperatures on post-settlement survival, that need to be considered to better understand variability in the adult stock and effectively support management of the fishery.

Conflict of Interest

The authors declare no conflicts of interest relevant to this study.

Availability Statement

The NEMO modeling framework is available at https://www.nemo-ocean.eu/ with the specific regional ocean model configuration available at https://github.com/emmafyoung/Tristan-da-Cunha. The HAL model is available at https://github.com/emmafyoung/HAL. Supporting data are available at https://doi.org/10.5281/zenodo.17258417.

Acknowledgments
This research was funded by NERC Grant NE/R000107/1 and the British Antarctic Survey National Capability PRESCIENT programme (UK Polar Expertise for Science and Society) NE/Y006178/1. Modeling studies were conducted on the British Antarctic Survey high performance computing facility and the ARCHER UK (www.archer.ac.uk) National Supercomputing Service. Simulated currents from global NEMO were provided by the National Oceanography Centre, Southampton, UK. Figure 1 was produced by Laura Gerrish of the Mapping and Geographic Information Centre, British Antarctic Survey.

References

Agardy, T. S. (1997). *Marine protected areas and Ocean conservation*. Academic Press. Retrieved from https://books.google.co.uk/books?id=BTh-kG4lz2wC

Belkin, I. M., & Gordon, A. L. (1996). Southern Ocean fronts from the Greenwich meridian to Tasmania. *Journal of Geophysical Research*, *101*(C2), 3675–3696. https://doi.org/10.1029/95JC02750

Bermudes, M., & Ritar, A. J. (2008). Response of early stage spiny lobster Jasus edwardsii phyllosoma larvae to changes in temperature and photoperiod. *Aquaculture*, *281*(1), 63–69. https://doi.org/10.1016/j.aquaculture.2008.05.035

Blamey, L. K., de Lecea, A. M., Jones, L. D. S., & Branch, G. M. (2019). Diet of the spiny lobster *Jasus paulensis* from the Tristan da Cunha archipelago: Comparisons between islands, depths and lobster sizes. *Estuarine, Coastal and Shelf Science*, *219*, 262–272. https://doi.org/10.1016/j.ecss.2019.02.021

Booth, J. D. (2006). Jasus species. In *Lobsters: Biology, management, aquaculture and fisheries* (pp. 340–358). John Wiley & Sons, Ltd. https://doi.org/10.1002/9780470995969.ch10

Bradford, R. W., Bruce, B. D., Chiswell, S. M., Booth, J. D., Jeffs, A., & Wotherspoon, S. (2005). Vertical distribution and diurnal migration patterns of *Jasus edwardsii* phyllosomas off the east coast of the North Island, New Zealand. *New Zealand Journal of Marine and Freshwater Research*, *39*(3), 593–604. https://doi.org/10.1080/00288330.2005.9517338

Bradford, R. W., Griffin, D., & Bruce, B. D. (2015). Estimating the duration of the pelagic phyllosoma phase of the southern rock lobster, Jasus edwardsii (Hutton). *Marine and Freshwater Research*, *66*(3), 213. https://doi.org/10.1071/MF14065

Burls, N. J., & Reason, C. J. C. (2006). Sea surface temperature fronts in the midlatitude South Atlantic revealed by using microwave satellite data. *Journal of Geophysical Research*, *111*(C8), 2005JC003133. https://doi.org/10.1029/2005JC003133

Byers, J. E. (2021). Marine parasites and disease in the era of global climate change. *Annual Review of Marine Science*, *13*(1), 397–420. https://doi.org/10.1146/annurev-marine-031920-100429

Cai, W., Borlace, S., Lengaigne, M., van Rensch, P., Collins, M., Vecchi, G., et al. (2014). Increasing frequency of extreme El Niño events due to greenhouse warming. *Nature Climate Change*, *4*(2), 111–116. https://doi.org/10.1038/nclimate2100

Campanella, F., Collins, M. A., Young, E. F., Laptikhovsky, V., Whomersley, P., & van der Kooij, J. (2021). First Insight of Meso- and bentho-pelagic fish dynamics around remote seamounts in the south Atlantic Ocean. *Frontiers in Marine Science*, *8*, 663278. https://doi.org/10.3389/fmars.2021.663278

Caputi, N., Fletcher, W. J., Pearce, A., & Chubb, C. F. (1996). Effect of the leeuwin current on the recruitment of fish and invertebrates along the Western Australian Coast. *Marine and Freshwater Research*, *47*(2), 147–155. https://doi.org/10.1071/mf9960147

Caselle, J. E., Hamilton, S. L., Davis, K., Bester, M., Wege, M., Thompson, C., et al. (2017). *Ecosystem Assessment of the Tristan Da Cunha Islands. National Geographic Pristine Seas*. Royal Society for Protection of Birds and Tristan da Cunha Government [Expedition Report].

Cetina-Heredia, P., Roughan, M., Van Sebille, E., Feng, M., & Coleman, M. A. (2015). Strengthened currents override the effect of warming on lobster larval dispersal and survival. *Global Change Biology*, *21*(12), 4377–4386. https://doi.org/10.1111/gcb.13063

Chiswell, S., & Booth, J. (1999). Rock lobster Jasus edwardsii larval retention by the Wairarapa Eddy off New Zealand. *Marine Ecology Progress Series*, *183*, 227–240. https://doi.org/10.3354/meps183227

Chiswell, S., & Booth, J. (2017). Evolution of long larval life in the Australasian rock lobster Jasus edwardsii. *Marine Ecology Progress Series*, *576*, 69–87. https://doi.org/10.3354/meps12233

Chiswell, S., Wilkin, J., Booth, J., & Stanton, B. (2003). Trans-Tasman Sea larval transport: Is Australia a source for New Zealand rock lobsters? *Marine Ecology Progress Series*, *247*, 173–182. https://doi.org/10.3354/meps247173

Chung, C. T. Y., Power, S. B., Boschat, G., Gillett, Z. E., & Narsey, S. (2024). Projected changes to characteristics of El niño-southern oscillation, Indian Ocean dipole, and Southern annular mode events in the CMIP6 models. *Earth's Future*, *12*(11), e2024EF005166. https://doi.org/10.1029/2024EF005166

Danovaro, R., Corinaldesi, C., Dell'Anno, A., Fuhrman, J. A., Middelburg, J. J., Noble, R. T., & Suttle, C. A. (2011). Marine viruses and global climate change. *FEMS Microbiology Reviews*, *35*(6), 993–1034. https://doi.org/10.1111/j.1574-6976.2010.00258.x

Deschamps, M., Giménez, L., Astley, C., Boersma, M., & Torres, G. (2025). Heatwave duration, intensity and timing as drivers of performance in larvae of a marine invertebrate. *Scientific Reports*, *15*(1), 15949. https://doi.org/10.1038/s41598-025-98259-7

Deshayes, J., Tréguier, A.-M., Barnier, B., Lecointre, A., Sommer, J. L., Molines, J.-M., et al. (2013). Oceanic hindcast simulations at high resolution suggest that the Atlantic MOC is bistable. *Geophysical Research Letters*, *40*(12), 3069–3073. https://doi.org/10.1002/grl.50534

Drouin, K. L., Lozier, M. S., & Johns, W. E. (2021). Variability and trends of the south Atlantic subtropical gyre. *Journal of Geophysical Research: Oceans*, *126*(1), e2020JC016405. https://doi.org/10.1029/2020JC016405

Dussin, R., Barnier, B., & Brodeau, L. (2016). The making of Drakkar forcing set DFS5 (DRAKKAR/MyOcean Report 01-04-16).

Dyke, P. (2001). *Coastal and shelf sea modelling*. Kluwer Academic.

Egbert, G. D., & Erofeeva, S. Y. (2002). Efficient inverse Modeling of barotropic ocean tides. *Journal of Atmospheric and Oceanic Technology*, *19*(2), 183–204. https://doi.org/10.1175/1520-0426(2002)019<0183:eimobo>2.0.co;2

Erickson, N. E., & Patricola, C. M. (2023). Future projections of the El Niño—Southern oscillation and tropical Pacific mean State in CMIP6. *Journal of Geophysical Research: Atmospheres*, *128*(21), e2022JD037563. https://doi.org/10.1029/2022JD037563

Fogarty, M. J., Sissenwine, M. P., & Cohen, E. B. (1991). Recruitment variability and the dynamics of exploited marine populations. *Trends in Ecology & Evolution*, *6*(8), 241–246. https://doi.org/10.1016/0169-5347(91)90069-a

Fogt, R. L., & Marshall, G. J. (2020). The Southern Annular Mode: Variability, trends, and climate impacts across the Southern Hemisphere. *WIREs Climate Change*, *11*(4), e652. https://doi.org/10.1002/wcc.652

Ford, D., Tilstone, G. H., Shutler, J. D., Kitidis, V., Lobanova, P., Schwarz, J., et al. (2021). Wind speed and mesoscale features drive net autotrophy in the South Atlantic Ocean. *Remote Sensing of Environment*, *260*, 112435. https://doi.org/10.1016/j.rse.2021.112435

Garcia-Soto, C., Cheng, L., Caesar, L., Schmidtko, S., Jewett, E. B., Cheripka, A., et al. (2021). An overview of Ocean climate change indicators: Sea surface temperature, Ocean Heat content, Ocean pH, dissolved oxygen concentration, Arctic Sea ice extent, thickness and volume, Sea level and strength of the AMOC (Atlantic meridional overturning circulation). *Frontiers in Marine Science*, *8*, 642372. https://doi.org/10.3389/fmars.2021.642372

GEBCO Compilation Group. (2025). *GEBCO 2025 Grid*. NERC EDS British Oceanographic Data Centre NOC. British Oceanographic Data Centre. https://doi.org/10.5285/37c52e96-24ea-67ce-e063-7086abc05f29

George, R. W. (2005). Review: Evolution of life cycles, including migration, in spiny lobsters (Palinuridae). *New Zealand Journal of Marine and Freshwater Research*, *39*(3), 503–514. https://doi.org/10.1080/00288330.2005.9517329

George, R. W., & Kensler, C. B. (1970). Recognition of marine spiny lobsters of the *Jasus lalandii* group (Crustacea: Decapoda: Palinuridae). *New Zealand Journal of Marine and Freshwater Research*, *4*(3), 292–311. https://doi.org/10.1080/00288330.1970.9515348

21699291, 2026, 7, Downloaded from https://agupubs.onlinelibrary.wiley.com/doi/10.1029/2025JC023603 by British Antarctic Survey, Wiley Online Library on [23/07/2026]. See the Terms and Conditions (https://onlinelibrary.wiley.com/terms-and-conditions) on Wiley Online Library for rules of use; OA articles are governed by the applicable Creative Commons License

Glass, J. P. (2014). *The fishery and biology of the rock lobster Jasus tristani at the Tristan da Cunha Islands group [Thesis]*. Cape Peninsula University of Technology. Retrieved from https://etd.cput.ac.za/handle/20.500.11838/2033

Graham, R. M., & De Boer, A. M. (2013). The dynamical subtropical front: The dynamical subtropical front. *Journal of Geophysical Research: Oceans*, *118*(10), 5676–5685. https://doi.org/10.1002/jgrc.20408

Graham, R. M., de Boer, A. M., Heywood, K. J., Chapman, M. R., & Stevens, D. P. (2012). Southern Ocean fronts: Controlled by wind or topography? *Journal of Geophysical Research*, *117*(C8). https://doi.org/10.1029/2012jc007887

Groeneveld, J. C., Von Der Heyden, S., & Matthee, C. A. (2012). High connectivity and lack of mtDNA differentiation among two previously recognized spiny lobster species in the southern Atlantic and Indian Oceans. *Marine Biology Research*, *8*(8), 764–770. https://doi.org/10.1080/17451000.2012.676185

Halpern, B. S., Walbridge, S., Selkoe, K. A., Kappel, C. V., Micheli, F., D'Agrosa, C., et al. (2008). A global map of human impact on marine ecosystems. *Science*, *319*(5865), 948–952. https://doi.org/10.1126/science.1149345

Hay, J. E. (2013). Small island developing states: Coastal systems, global change and sustainability. *Sustainability Science*, *8*(3), 309–326. https://doi.org/10.1007/s11625-013-0214-8

Hinojosa, I. A., Green, B. S., Gardner, C., Hesse, J., Stanley, J. A., & Jeffs, A. G. (2016). Reef sound as an orientation cue for shoreward migration by Pueruli of the rock lobster, Jasus edwardsii. *PLoS One*, *11*(6), e0157862. https://doi.org/10.1371/journal.pone.0157862

Hobday, A. J., & Pecl, G. T. (2014). Identification of global marine hotspots: Sentinels for change and vanguards for adaptation action. *Reviews in Fish Biology and Fisheries*, *24*(2), 415–425. https://doi.org/10.1007/s11160-013-9326-6

Hochachka, P. W. & Somero, G. N. (Eds.) (2002). *Biochemical adaptation: Mechanism and process in physiological evolution*. Oxford University Press. https://doi.org/10.1093/oso/9780195117028.002.0001

Johnston, S. (2025). *Tristan Group Biomass Survey results of Jasus tristani including data from the 2024 season (Report)*. University of Cape Town. https://doi.org/10.25375/uct.28759313.v1

Lubchenco, J., Palumbi, S. R., Gaines, S. D., & Andelman, S. (2003). Plugging a hole in the Ocean: The emerging science of marine reserves. *Ecological Applications*, *13*(1), S3–S7. https://doi.org/10.1890/1051-0761(2003)013[0003:pahito]2.0.co;2

Marcello, F., Tonelli, M., Ferrero, B., & Wainer, I. (2023). Projected Atlantic overturning slow-down is to be compensated by a strengthened South Atlantic subtropical gyre. *Communications Earth & Environment*, *4*(1), 92. https://doi.org/10.1038/s43247-023-00750-4

Marochi, M. Z., De Grande, F. R., Farias Pardo, J. C., Montenegro, Á., & Costa, T. M. (2022). Marine heatwave impacts on newly-hatched planktonic larvae of an estuarine crab. *Estuarine, Coastal and Shelf Science*, *278*, 108122. https://doi.org/10.1016/j.ecss.2022.108122

Marzocchi, A., Hirschi, J. J.-M., Holliday, N. P., Cunningham, S. A., Blaker, A. T., & Coward, A. C. (2015). The North Atlantic subpolar circulation in an eddy-resolving global ocean model. *Journal of Marine Systems*, *142*, 126–143. https://doi.org/10.1016/j.jmarsys.2014.10.007

Micheli, F., Saenz-Arroyo, A., Greenley, A., Vazquez, L., Montes, J. A. E., Rossetto, M., & Leo, G. A. D. (2012). Evidence that marine reserves enhance resilience to climatic impacts. *PLoS One*, *7*(7), e40832. https://doi.org/10.1371/journal.pone.0040832

Monteiro, M., De Castro, S. L. P., Marques, S. C., Freitas, R., & Azeiteiro, U. M. (2023). An emergent treat: Marine heatwaves—Implications for marine decapod crustacean species—An overview. *Environmental Research*, *229*, 116004. https://doi.org/10.1016/j.envres.2023.116004

Morgan, S. G., Fisher, J. L., & Largier, J. L. (2011). Larval retention, entrainment, and accumulation in the lee of a small headland: Recruitment hotspots along windy coasts. *Limnology and Oceanography*, *56*(1), 161–178. https://doi.org/10.4319/lo.2011.56.1.0161

Morley, S. A., Campanella, F., Young, E. F., Baylis, A. M. M., Barnes, D. K. A., Bell, J. B., et al. (2025). Dramatic ENSO related southwestern Atlantic ecosystem shifts. *Scientific Reports*, *15*(1), 7917. https://doi.org/10.1038/s41598-025-93080-8

Morley, S. A., Collins, M. A., Barnes, D. K. A., Sands, C., Bell, J., Walmsley, S., et al. (2018). Helping Tristan da Cunha and St Helena manage their marine environments. Report of James Clark Ross cruise 17-004. (Cruise Summary Report No. 16779) (pp. 1–139). Retrieved from https://www.bodc.ac.uk/resources/inventories/cruise_inventory/report/16779/

Myers, R. A., & Pepin, P. (1994). Recruitment variability and oceanographic stability. *Fisheries Oceanography*, *3*(4), 246–255. https://doi.org/10.1111/j.1365-2419.1994.tb00102.x

Oregon State University, IUCN World Commission on Protected Areas—Marine, Marine Conservation Institute, National Geographic Pristine Seas, and UN Environment Programme World Conservation Centre. (2023). The MPA Guide User Manual, version 1. Retrieved from https://mpa-guide.protectedplanet.net

Park, Y.-H., & Durand, I. (2019). Altimetry-drived Antarctic Circumpolar Current fronts [Dataset]. *SEANOE*. https://doi.org/10.17882/59800

Peng, Q., Xie, S.-P., Wang, D., Huang, R. X., Chen, G., Shu, Y., et al. (2022). Surface warming–induced global acceleration of upper ocean currents. *Science Advances*, *8*(16), eabj8394. https://doi.org/10.1126/sciadv.abj8394

Pollock, D. E. (1986). Review of the fishery for and biology of the cape rock lobster Jasus lalandii with notes on larval recruitment. *Canadian Journal of Fisheries and Aquatic Sciences*, *43*(11), 2107–2117. https://doi.org/10.1139/f86-259

Pollock, D. E. (1990). Palaeoceanography and speciation in the Spiny Lobster Genus Jasus. *Bulletin of Marine Science*, *46*(2), 387–405.

Pollock, D. E. (1991). Spiny lobsters at Tristan da Cunha, South Atlantic: Inter-island variations in growth and population structure. *South African Journal of Marine Science*, *10*(1), 1–12. https://doi.org/10.2989/02577619109504614

Roscoe, M. J. (1979). Biology and exploitation of the rock lobster Jasus tristani at the Tristan da Cunha Islands. In *South Atlantic, 1949-1976 (No. 118; investigational report Sea fisheries branch South Africa)* (pp. 1–47).

Ryan, W. B. F., Carbotte, S. M., Coplan, J. O., O'Hara, S., Melkonian, A., Arko, R., et al. (2009). Global Multi-Resolution Topography synthesis. *Geochemistry, Geophysics, Geosystems*, *10*(3). https://doi.org/10.1029/2008GC002332

Sala, E., & Giakoumi, S. (2018). No-take marine reserves are the most effective protected areas in the ocean. *ICES Journal of Marine Science*, *75*(3), 1166–1168. https://doi.org/10.1093/icesjms/fsx059

Sánchez-Llamas, E., & Groeneveld, J. (2025). Marine Stewardship Council (MSC) 3rd Surveillance Audit: Tristan da Cunha Rock Lobster.

Sérazin, G., Penduff, T., Grégorio, S., Barnier, B., Molines, J.-M., & Terray, L. (2015). Intrinsic variability of Sea level from Global Ocean simulations: Spatiotemporal scales. *Journal of Climate*, *28*(10), 4279–4292. https://doi.org/10.1175/JCLI-D-14-00554.1

Silva, C. N. S., Young, E. F., Murphy, N. P., Bell, J. J., Green, B. S., Morley, S. A., et al. (2021). Climatic change drives dynamic source–sink relationships in marine species with high dispersal potential. *Ecology and Evolution*, *11*(6), 2535–2550. https://doi.org/10.1002/ece3.7204

Smale, D. A., Wernberg, T., Oliver, E. C. J., Thomsen, M., Harvey, B. P., Straub, S. C., et al. (2019). Marine heatwaves threaten global biodiversity and the provision of ecosystem services. *Nature Climate Change*, *9*(4), 306–312. https://doi.org/10.1038/s41558-019-0412-1

Smythe-Wright, D., Chapman, P., Rae, C. D., Shannon, L. V., & Boswell, S. M. (1998). Characteristics of the South Atlantic subtropical frontal zone between 15°W and 5°E. *Deep Sea Research Part I: Oceanographic Research Papers*, *45*(1), 167–192. https://doi.org/10.1016/S0967-0637(97)00068-X

Stanley, J. A., Hesse, J., Hinojosa, I. A., & Jeffs, A. G. (2015). Inducers of settlement and moulting in post-larval spiny lobster. *Oecologia*, *178*(3), 685–697. https://doi.org/10.1007/s00442-015-3251-4

21699291, 2026, 7, Downloaded from https://agupubs.onlinelibrary.wiley.com/doi/10.1029/2025JC023603 by British Antarctic Survey, Wiley Online Library on [23/07/2026]. See the Terms and Conditions (https://onlinelibrary.wiley.com/terms-and-conditions) on Wiley Online Library for rules of use; OA articles are governed by the applicable Creative Commons License

Trathan, P. N., Warwick-Evans, V., Young, E. F., Friedlaender, A., Kim, J. H., & Kokubun, N. (2022). The ecosystem approach to management of the Antarctic krill fishery—The 'devils are in the detail' at small spatial and temporal scales. *Journal of Marine Systems*, *225*, 103598. https://doi.org/10.1016/j.jmarsys.2021.103598

Twiname, S., Fitzgibbon, Q., Hobday, A., Carter, C., Oellermann, M., & Pecl, G. (2022). Resident lobsters dominate food competition with range-shifting lobsters in an ocean warming hotspot. *Marine Ecology Progress Series*, *685*, 171–181. https://doi.org/10.3354/meps13984

Vianna, M. L., & Menezes, V. V. (2011). Double-celled subtropical gyre in the South Atlantic Ocean: Means, trends, and interannual changes. *Journal of Geophysical Research*, *116*(C3), C03024. https://doi.org/10.1029/2010JC006574

Von Der Heyden, S., Groeneveld, J., & Matthee, C. (2007). Long current to nowhere?—Genetic connectivity of Jasus tristani populations in the southern Atlantic Ocean. *African Journal of Marine Science*, *29*(3), 491–497. https://doi.org/10.2989/ajms.2007.29.3.15.345

Vye, S. R., Lavarello, J., Glass, T., Glass, J., Escobar-Porras, J., & Schofield, A. (2024). Adaptive, flexible and community-led: Management support for the largest fully protected marine area in the Atlantic. *Marine Policy*, *167*, 106284. https://doi.org/10.1016/j.marpol.2024.106284

Wang, G., Cai, W., Gan, B., Wu, L., Santoso, A., Lin, X., et al. (2017). Continued increase of extreme El Niño frequency long after 1.5°C warming stabilization. *Nature Climate Change*, *7*(8), 568–572. https://doi.org/10.1038/nclimate3351

Whomersley, P., Morley, S., Bell, J., Collins, M., Pettafor, A., Campanella, F., et al. (2019). RRS Discovery 100 survey report: Marine Biodiversity of Tristan da Cunha and St Helena (Cruise Summary Report No. 17220) (pp. 1–124). Retrieved from https://www.bodc.ac.uk/resources/inventories/cruise_inventory/report/17220/

Wilson, L. J., Fulton, C. J., Hogg, A. M., Joyce, K. E., Radford, B. T. M., & Fraser, C. I. (2016). Climate-driven changes to ocean circulation and their inferred impacts on marine dispersal patterns. *Global Ecology and Biogeography*, *25*(8), 923–939. https://doi.org/10.1111/geb.12456

Yang, H., Lohmann, G., Krebs-Kanzow, U., Ionita, M., Shi, X., Sidorenko, D., et al. (2020). Poleward shift of the major Ocean gyres detected in a warming climate. *Geophysical Research Letters*, *47*(5), e2019GL085868. https://doi.org/10.1029/2019GL085868

Young, E. F. (2024). HAL (version v1.0) [Computer software]. *Zenodo*. https://doi.org/10.5281/zenodo.13760306

Young, E. F., Belchier, M., Hauser, L., Horsburgh, G. J., Meredith, M. P., Murphy, E. J., et al. (2015). Oceanography and life history predict contrasting genetic population structure in two Antarctic fish species. *Evolutionary Applications*, *8*(5), 486–509. https://doi.org/10.1111/eva.12259

Young, E. F., Thorpe, S. E., Banglawala, N., & Murphy, E. J. (2014). Variability in transport pathways on and around the South Georgia shelf, Southern Ocean: Implications for recruitment and retention. *Journal of Geophysical Research: Oceans*, *119*(1), 241–252. https://doi.org/10.1002/2013JC009348

Young, E. F., Thorpe, S. E., Renner, A. H. H., & Murphy, E. J. (2024). Environmental and behavioural drivers of Antarctic krill distribution at the South Orkney Islands: A regional perspective. *Journal of Marine Systems*, *241*, 103920. https://doi.org/10.1016/j.jmarsys.2023.103920

Young, E. F., Tysklind, N., Meredith, M. P., de Bruyn, M., Belchier, M., Murphy, E. J., & Carvalho, G. R. (2018). Stepping stones to isolation: Impacts of a changing climate on the connectivity of fragmented fish populations. *Evolutionary Applications*, *11*(6), 978–994. https://doi.org/10.1111/eva.12613

References From the Supporting Information

Edwards, K. P., Barciela, R., & Butenschom, M. (2012). Validation of the NEMO-ERSEM operational ecosystem model for the North West European Continental Shelf. *Ocean Science*, *8*(6), 983–1000. https://doi.org/10.5194/os-8-983-2012

Reynolds, R. W., Rayner, N. A., Smith, T. M., Stokes, D. C., & Wang, W. (2002). An improved in situ and satellite SST analysis for climate. *Journal of Climate*, *15*(13), 1609–1625. https://doi.org/10.1175/1520-0442(2002)015<1609:AIISAS>2.0.CO;2

21699291, 2026, 7, Downloaded from https://agupubs.onlinelibrary.wiley.com/doi/10.1029/2025JC023603 by British Antarctic Survey, Wiley Online Library on [23/07/2026]. See the Terms and Conditions (https://onlinelibrary.wiley.com/terms-and-conditions) on Wiley Online Library for rules of use; OA articles are governed by the applicable Creative Commons License